Inhibition of H3K27me-Specific Demethylase Activity During Murine ES cell Differentiation Induces DNA Damage Response

Inhibierung der H3K27me-Spezifischen Demethylase Aktivität in Differenzierenden ES Zellen der Maus Induziert eine DNA Schadensantwort

Dissertation zur Erlangung des
Naturwissenschaftlichen Doktorgrades
der Julius-Maximilians-Universität Würzburg
vorgelegt von

Diplom Biologin

Christine Hofstetter

aus Köln

Würzburg, August 2014

Submitted on: _____

Office stamp

Members of the Promotionskomitee:

Chairperson:

Primary Supervisor: Prof. Dr. Albrecht Müller

Supervisor (Second): Prof. Dr. Ricardo Benavente

Date of Public Defence: _____

Date of Receipt of Certificate: _____

Table of Content

Summary

Pluripotent embryonic stem (ES) cells can renew indefinitely while keeping the potential to differentiate into any of the three germ layers (ectoderm, endoderm or mesoderm). For decades, ES cells are in the focus of research because of these unique features. When ES cells differentiate they form spheroid aggregates termed “embryoid bodies” (EBs). These EBs mimic post-implantation embryonic development and therefore facilitate the understanding of developmental mechanisms. During ES cell differentiation new genetic programs get activated. This is accompanied by changes in the chromatin structure. In ES cells, several mechanisms are involved in the regulation of the chromatin architecture, including post-translational modifications of histones. In recent years histone methylation marks became one of the best-investigated epigenetic modifications, in part because of their relevance for the maintenance of pluripotency. Until the first histone demethylase KDM1A was discovered in 2004 histone modifications were considered to be irreversible. Since then, a great number of histone demethylases have been identified. Their activity is linked to gene regulation as well as to stem cell self-renewal and differentiation. KDM6A and KDM6B are H3K27me3/2-specific histone demethylases, which are known to play a central role in the regulation of body axis specification by regulating HOX gene expression profiles. So far little is known about the molecular functions of KDM6A or KDM6B in undifferentiated and differentiating ES cells. In order to completely abrogate KDM6A and KDM6B demethylase activities, a specific inhibitor (GSK-J4) was employed. Treatment with GSK-J4 had no effect on the viability or proliferation of undifferentiated ES cells. However, in the presence of GSK-J4, ES cell differentiation was completely abrogated with cells arrested in G1-phase and an increased rate of apoptosis. Global transcriptome analyses in early-differentiating ES cells revealed that only a limited set of genes were differentially regulated in response to GSK-J4 treatment with more genes up-regulated than down-regulated. Many of the up-regulated genes are linked to DNA damage response (DDR). In agreement with this, DNA damage was found in EBs incubated with GSK-J4. A co-localization of H3K27me3 or KDM6B with γH2AX foci, marking DNA breaks, could be excluded. However, differentiating Eed knockout (KO) ES cells, which are devoid of the H3K27me3 mark, showed an attenuated GSK-J4-induced DDR. Finally,

hematopoietic differentiation in the presence of GSK-J4 resulted in a reduced colony-forming potential. This leads to the conclusion that differentiation in the presence of GSK-J4 is not solely restricted to ES cell differentiation.

In conclusion, my results show that the enzymatic activity of KDM6A and KDM6B is not essential for maintaining the pluripotent state of ES cells. In contrast, the enzymatic activity of both proteins is indispensable for ES cell and hematopoietic differentiation. Additionally KDM6A and KDM6B enzymatic inhibition in differentiating ES cells leads to increased DNA damage with an activated DDR. Therefore, KDM6A and KDM6B are associated in differentiating ES cells with DNA damage and in DDR.

Zusammenfassung

Pluripotente embryonale Stammzellen (ES Zellen) können sich fortlaufend erneuern und besitzen zudem das Potential, in alle drei Keimblätter (Ektoderm, Endoderm oder Mesoderm) zu differenzieren. Auf Grund dieser einzigartigen Eigenschaften sind ES Zellen seit Jahrzehnten im Focus der Wissenschaft. Wenn ES Zellen differenzieren, sind sie in der Lage, sphäroid-förmige Aggregate zu bilden, welche als embryoide Körperchen (EBs) bezeichnet werden. In EBs finden sich Zellen aller 3 Keimblätter und daher dienen sie als *in vitro* Modell für frühe embryonale Entwicklung. Während der ES Zell Differenzierung werden neue genetische Programme aktiviert. Diese gehen mit Veränderungen der Chromatinstruktur einher. ES Zellen besitzen eine Vielzahl von Mechanismen, die mit der Regulation des Chromatins assoziiert sind, einschließlich der post-translationalen Modifikation von Histonen. Post-translationale Histon-methylierung gehören zu den am häufigsten untersuchten epigenetischen Modifikationen und spielen z.B. ein wichtige Rolle bei der Aufrechterhaltung der Pluripotenz. Bis zur Entdeckung der ersten Histon-Demethylase KDM1A im Jahre 2004 glaubte man, dass Modifikationen an Histonen irreversible sind. Bislang wurden eine Vielzahl weiterer Histon-Demethylasen identifiziert, welche mit der Genregulation, sowie der Selbsterneuerung und Differenzierung von Stammzelle in Verbindung gebracht werden konnten. Die H3K27me3/2-spezifischen Histon-Demethylasen KDM6A und KDM6B regulieren Hox Gene, welche bei der Festlegung der Körperachse eine wichtige Rolle spielen. Bislang ist über die molekulare Funktion von KDM6A und KDM6B in nicht differenzierten und differenzierenden ES Zellen wenig bekannt. Um die KDM6A und KDM6B Demethylase Aktivität außer Kraft zu setzten kam ein spezifischer Inhibitor (GSK-J4) zum Einsatz. Die Behandlung mit GSK-J4 zeigte keine Auswirkungen auf die Lebensfähigkeit oder Proliferation von nicht differenzierten ES Zellen. Jedoch war die Differenzierung von ES Zellen in Gegenwart von GSK-J4 inhibiert und zeigte einen erhöhten G1-Phase Arrest sowie eine erhöhte Rate an apoptotischen Zellen. Eine globale Transkriptionsanalyse in frühen differenzierenden ES Zellen, in Gegenwart von GSK-J4 zeigte, dass lediglich eine relativ geringe Zahl von Genen differenziell reguliert war. Dabei waren mehr Gene hochreguliert als

herunterreguliert. Viele der hochregulierten Gene konnten mit der DNA Schadensantwort in Verbindung gebracht werden. In Übereinstimmung damit konnte in Gegenwart von GSK-J4 in differenzierenden ES Zellen DNA Schaden nachgewiesen werden. Eine Kolokalisation von H3K27me3 oder KDM6B mit γH2AX markierten Foci, welche DNA Schaden markieren, konnte nicht nachgewiesen werden. Nichts desto trotz zeigten GSK-J4 behandelte, differenzierende Eed KO ES Zellen, welche keine H3K27me3 Modifikation besitzen, eine abgemilderte DNA Schadensantwort. In Anwesenheit von GSK-J4 konnte während der hämatopoetischen Differenzierung eine reduzierte Kolonie-Bildung beobachtet werden. Daraus lässt sich schließen, dass in Anwesenheit von GSK-J4 nicht ausschließlich die ES Zell Differenzierung inhibiert wird.

Zusammenfassend zeigen meine Ergebnisse, dass die enzymatische Aktivität von KDM6A und KDM6B für die Aufrechterhaltung des pluripotenten Zustands nicht essenziell ist. Im Gegensatz dazu ist die enzymatische Aktivität beider Proteine unabdingbar für die ES Zell sowie die hämatopoetische Differenzierung. Die enzymatische Inhibierung von KDM6A und KDM6B führt während der Differenzierung zu einem erhöhten DNA Schaden, wodurch die DNA Schadensantwort aktiviert wird. Somit sind KDM6A und KDM6B in differenzierenden ES Zellen mit DNA Schaden und der DNA Schadensantwort assoziiert.

1. Introduction

1.1 Stem Cells

Stem cells are rare cell types that constitute multicellular organism. They possess two main functional characteristics: self-renewing and multilineage differentiation [1, 2]. Based on these two functional characteristics stem cells are essential for the generation and homeostasis of diverse tissues and they are attractive tools for basic and applied research.

Mammalian development starts with the fertilisation of an oocyte by a sperm forming the zygote. The zygote is a totipotent cell type which is defined by its potential to develop into an embryo with all the specialized cells needed for a living organism [3]. Totipotent cells possess the potential to develop into placental support structures, termed trophoblast, and are able to differentiate into cells of the three germ layers: ectoderm, endoderm or mesoderm; which in total are necessary for implantation, embryonic development and germ cells. Totipotency applies to the zygote and to early blastomeres, which develop from the zygote by cell division. Totipotent cells have the highest developmental potential for differentiation [3]. Mouse embryonic stem (ES) cells are derived from the inner cell mass (ICM) of a developing blastocyst: a stage of the pre-implantation embryo 3.5 days post-fertilization [1]. Pluripotent ES cells are able to differentiate into each of the three primary germ layers and, when introduced into the pre-implantation embryo, they can generate chimeras [3]. Specialized stem cell types, known as somatic or adult stem cells, can be found in post-implantation and in differentiated tissues. Their primary role is to maintain tissue homeostasis and repair injured tissues. Adult stem cells like hematopoietic, neural, mesenchymal or epithelial stem cells show less differentiation potential compared to toti- or pluripotent stem cells as they generate only differentiated progeny of their stem cell system [4].

In multi-cellular organisms, stem cells reside in the so-called stem cell niche [5]. Stem cell niches play fundamental roles in the protection and maintenance of stem cells. The architectural design of a niche is versatile and influences the proliferation and differentiation status on the stem cells. Stem cell niches share similarities in activating common signal transduction pathways to achieve the self-renewal and

undifferentiated state of their residence. Signals from the microenvironment of the niche also trigger stem cell division [5]. Two basic modes of stem cell division, the symmetrical and asymmetrical mode, are discussed. Symmetric division results in a dividing stem cell where either both daughter cells keep the stem cell potential or both daughter cells generate differentiating cells. An asymmetrically division results when one daughter cell generates differentiating cells and one daughter cell keeps the stem cell potential [6].

1.1.1 Mouse Embryonic Stem Cells

In the early 1980's, ES cells were first derived from the ICM of inbred mouse strains [1, 2]. Since then, pluripotent ES cells were successfully isolated from humans, primates, rats and other mammalian species [7-10]. Maintaining the pluripotent state in an ES cell culture is achieved through the prevention of ES cell differentiation. The leukemia inhibitory factor (LIF), which is added to the culture medium, is the main factor for keeping murine ES cells pluripotent [11, 12]. Additionally high concentrations of fetal calf serum (FCS) and the co-culturing of murine ES cells on a supportive layer of mouse embryonic fibroblasts (MEFs) favours the maintenance of the pluripotent state [11, 12]. The cytokine LIF promotes the self-renewal and pluripotent phenotype of ES cells through activation of STAT3 (signal transducer and activator of transcription 3) signalling by binding to heterodimers of the LIF-receptor and the signal transducer gp130 [13]. Activated STAT3 dimers are transported into the nucleus where they bind to promoter and enhancer regions of target genes (*e.g.,* Oct3/4, Nanog and Sox2) [14-16]. Several analyses can be performed to determine if ES cells maintain pluripotency over time when in culture. The pluripotent state is morphologically characterised by tightly associated cells growing in rounded clusters [17]. Additionally, pluripotent ES cells exhibit an unusual cell cycle phase distribution, characterized by a short G1-phase and a high proportion of cells in S-phase [18]. Furthermore ES cells form a homogeneous cell population [2]. An *in vivo* differentiation by injecting ES cells subcutaneous into mice forming teratoma can be performed to determine ES cell pluripotency. A teratoma is a multi-cellular tumour mass with cells from all germ layers [19]. The 'golden standard' to determine ES cell

pluripotency is however the injection of ES cells into blastocysts where they form germ line-competent chimeras [20].

Molecularly, ES cells can be characterised by the expression of several markers. Most common markers are the core transcription factors Oct3/4, Nanog and Sox2, which are essential to maintain the pluripotent state and cell identity of ES cells [21, 22]. Oct3/4, Nanog and Sox2 are central players in a transcriptional network that on one side activate genes necessary for survival while on the other side help to repress genes that are involved in differentiation [21-26]. In undifferentiated ES cells Oct3/4, Nanog and Sox2 are highly expressed while upon differentiation they get downregulated [21].

The capacity of ES cells to differentiate into derivatives of all three germ layers and germ cells is assessed in various ways [12, 27-29]. *In vitro* differentiation can be achieved through the formation of so-called embryoid bodies (EBs) [30]. These structures are formed when ES cells are grown in drops hanging from the lid of a Petri-dish or upon culture of ES cells in non-adherent dishes. Aggregated ES cells start to differentiate and recapitulate embryonic development to a limited extent, thereby forming derivatives of all three embryonic layers [3]. ES cells and differentiating ES cells are preferentially used for applied research since they represent a fast alternative to study gene functions involved in pluripotency and upon ES cell differentiation [31].

1.2 Epigenetic Modifications

The term ‘Epigenetic’ is defined as the sum of processes which cause heritable and reversible changes of gene expression patterns that do not involve changes of the DNA sequence itself [32]. Epigenetic modifications are *e.g.* the methylation of DNA, RNA and histones. An epigenetic modification enzyme is, for instance, DNA methyltransferase (DNMT), which methylates cytosine to 5-methylcytosine (5mC) within cytosine-guanine dinucleotides (CpG) [33]. The methylated DNA mark serves as a binding site for methyl-CpG-binding domain (MBD) proteins. MBD recruits chromatin modifying proteins and complexes, which are associated with gene silencing or gene activation.

Additional epigenetic modifications consist of a multitude of post-transcriptional modifications of messenger RNA (mRNA) and long non-coding RNA (lncRNA). mRNAs are coding for proteins while lncRNA are non-protein coding transcripts that regulate gene expression on transcriptional and post-transcriptional level by targeting either local or distant genes. Both RNA molecule classes can be modified and can effect mRNA splicing, transport, stability and immune tolerance [34].
Furthermore, epigenetic mechanisms comprise of modifications of histones. These modifications, catalysed by histone modifying enzymes, are associated with activation or repression of transcription states depending on the histone residue that gets modified [35].
Most DNA, RNA or histone modifications are reversible and can be removed either passively or actively. Passive removal of epigenetic modifications occurs during the cell cycle following DNA replication where the newly synthesized strand lacks the epigenetic mark. Active removal of modifications involves one or more enzymes that remove specific modifications independently of DNA replication [36].

1.2.1 Post-translational Histone Modifications

In eukaryotic organisms the DNA, with the exception of the mitochondrial DNA, is packed into the nucleus. The nucleus, with a diameter of ~10 µm, covers a relatively small fraction of the whole cell volume. The total length of a haploid set of human chromosomes is about 2 meters long. To make the genetic material fit into the nucleus several levels of packaging are needed. The first packaging step is the wrapping of the DNA around a histone octamer to form the so-called nucleosome [37]. Within this nucleosome, ~146 bp of the DNA are wrapped around this protein octamer, which contains two copies of each core histone named H2A, H2B, H3 and H4. Histones are evolutionarily conserved proteins, which form with the genetic material: a nucleo-protein complex termed chromatin [38].
Two types of chromatin are distinguished: euchromatin and heterochromatin. Euchromatin is less condensed, gene-rich and more accessible for transcription while heterochromatin is typically highly condensed, gene-poor and transcriptionally silent [39]. A further distinction is made between constitutive and facultative heterochromatin. Constitutive heterochromatin domains are often found at

centromeres, telomeres and repetitive sequences and are largely transcriptionally silent. Unlike facultative heterochromatin, constitutive heterochromatin is not converted back into euchromatin [22, 40].

Histones and in particular, N-terminal histone tails, are subject to a multitude of post-translational modifications. Histone tail modifications identified so far comprise acetylation, methylation, phosphorylation, ubiquitylation, sumoylation and ADP ribosylation [41-46]. Some post-translational modifications on histone tails result in gene repression (*e.g.,* sumoylation) while other modifications lead to gene activation (*e.g.,* acetylation, phosphorylation) [47]. Some histone tail modifications also serve as platforms for protein complexes, which further modify histone tails (*e.g.,* Polycomb Repressive Complex 2 (PRC2)) and are associated with gene activation or repression. Among the most common and best-investigated modifications are acetylation and methylation of lysine (K) and arginine (R) residues. Histone tail acetylation neutralize the positive charge of the lysine/arginine residues of the histones, thus weakening their interaction with the nucleosomal DNA which further leads to a more open chromatin structure which facilitates the access of transcription factors to their recognition elements [48, 49]. Contrary to acetylation the charge of histone tail residues is not altered upon methylation and therefore, DNA-histone interactions are not altered [48].

1.2.1.1 Histone Methyltransferases and Demethylases

Further histone modifying enzymes, which influence gene expression, are histone methyltransferases (HMTs) and histone demethylases (HDMs). HMTs and HDMs often function in one multiprotein complex that methylates one residue while demethylating another residue. Well-investigated complexes are the Trithorax group (TrxG) complex and the PRC2 complex [50]. Histone tail methylations appear either on lysine or arginine of histone H3 (K4, K9, K27, K36, R2, R26) or H4 (K20, R3) and have impact on gene repression or activation [51]. HMTs can further be grouped into protein arginine methyltransferases (PRMTs) and histone lysine methyltransferases (HKMTs).

In vivo, methylated lysine can be found either in a mono-, di-, or trimethylated state, whereas arginine can either be mono- or dimethylated [52]. The extent of methylation at specific residues is important for the recognition of effector proteins and has impact on the chromatin compaction and the transcription status [50]. Histone methylation is normally mediated through the recruitment of methylation-specific binding proteins. Four major protein subdomains that are capable of binding to methylated lysine are identified as the chromodomain, the Tudor domain, the WD40 domain and the PHD domain. Most lysine methyltransferases contain one or more of these domains [53]. Three families of enzymes are capable of methylating histones: the PRMT family, which methylate arginine residues, the SET-domain and the non-SET-domain families, which are both capable of methylating lysine residues [53, 54]. These enzymes add methyl marks to lysine and arginine residues predominantly on the N-terminal tails of histones [53]. Histone methylation marks were for a long time thought to be irreversible because of the high thermodynamic stability of the N-CH_3 bond [50].

The discovery of the first histone lysine demethylase (KDM1A) in 2004 opened new avenues for the understanding of how histone methylation impacts cellular functions [55]. Since then many histone lysine demethylases (Table 1) and histone arginine demethylases have been identified [50]. Histone lysine demethylases are divided into two groups. Members of the KDM1 family belong to a group of proteins, which are flavin adenine dinucleotide (FAD)-dependent. These proteins demethylate histones in a FAD-dependent oxidative reaction, while oxidizing the methyl-lysine to lysine and formaldehyde [56]. KDM2 to KDM8 family members contain a conserved Jumonji C (JmjC) catalytic domain, which drives the demethylase reaction [50, 55]. The family members of KDM2 to KDM8 require the cofactors Fe^{2+} and α-ketoglutarate. In the presence of oxygen, they oxidise methyl groups to hydroxymethyl by releasing formaldehyde [56].

Table 1: The growing family of lysine-specific demethylases
(modified from Nottke *et al.* [51])

family name	sub-family name	substrate specificity
KDM1	KDM1A (LSD1)	H3K4me2/1; H3K9me2/1
	KDM1B (LSD2)	H3K4me2/1
KDM2	KDM2A (Jhdm1A)	H3K36me2/1
	KDM2B (Jhdm1B)	H3K36me2/1; H3K4me3?
KDM3	KDM3A (Jmjd1A)	H3K9me2/1
	KDM3B (Jmjd1B)	H3K9me2/1
	KDM3C (Jmjd1C)	H3K9me2/1
KDM4	KDM4A (Jmjd2A)	H3K36me3/2; H3K9me3/2
	KDM4B (Jmjd2B)	H3K36me3/2; H3K9me3/2
	KDM4C (Jmjd2C)	H3K36me3/2; H3K9me3/2
	KDM4D (Jmjd2D)	H3K36me3/2; H3K9me3/2
KDM5	KDM5A (Jarid1A)	H3K4me3/2
	KDM5B (Jarid1B)	H3K4me3/2
	KDM5C (Jarid1C)	H3K4me3/2
	KDM5D (Jarid1D)	H3K4me3/2
KDM6	KDM6A (UTX)	H3K27me3/2
	KDM6B (Jmjd3)	H3K27me3/2
	KDM6C (UTY)	H3K27me3/2
KDM7	KDM7A (Jhdm1D)	H3K27me2; H3K9me2/1
KDM8	KDM8A (Jmjd5)	H3K36me2

The first JmjC catalytic domain was discovered in the protein JARID2 (Jumonji, AT rich interactive domain 2), which was later found to interact with PRC2 [57]. The term ‘Jumonji’ originates from Japanese and means cruciform. Takeuchi *et al.* used this term for mice developing an abnormal cross-like neural tube resulting from a genetrap inserted into the Jumonji locus of the JARID2 gene [58]. To date more than 100 JmjC-domain-containing proteins are identified in prokaryotic and eukaryotic organisms [59]. Thus far approximately 30 proteins, containing a JmjC domain, were identified in the human genome. A histone demethylase activity for lysine residues has been verified for more than 20 of them [60]. Although JARID2 contains a JmjC domain it lacks demethylase activity [61]. Histone lysine demethylases are linked to gene regulation as well as to stem cell self-renewal and differentiation [62]. In addition, alterations of the expression patterns as well as deletions, translocations and gene mutations of KDMs are associated with many types of cancer [63-69]. With this, KDMs represent a diagnostic tool and therapeutic target in the field of oncology.

1.3 H3K27me3/2-Specific Lysine Demethylases

In 1998, Greenfield and colleagues first described the murine protein UTX (ubiquitously transcribed TPR gene on the X chromosome) [70]. By this time, Greenfield had already proposed that although UTX is located on the X chromosome, it escapes X chromosome inactivation [70]. UTY (ubiquitously transcribed TPR gene on the Y chromosome) resides on the Y chromosome and is the male counterpart of UTX [71]. In contrast to UTX and UTY, the Jmjd3 (Jumonji D3) gene is encoded in an autosome on chromosome 11 in mice [72]. In 2007, a demethylase activity for UTX and Jmjd3 was described. Both enzymes catalyse the transition of H3K27me3 and, *in vitro*, also H3K27me2 to H3K27me1 [35, 73-75]. Just recently *in vitro* findings support the notion that UTY also has demethylase activity by catalysing the transition of H3K27me3 and H3K27me2 to H3K27me1 [76]. The activity of KDM6A and KDM6B contributes to gene activation through removal of H3K27me3/2 histone modification marks [77]. The newly discovered demethylase activities led to a change of the nomenclature of all known histone lysine demethylases. Hence UTX was renamed KDM6A, Jmjd3 KDM6B and UTY KDM6C. All three enzymes are members of the KDM6 family and possess a Jumonji C domain [73, 78-80]. KDM6A and KDM6C additionally contain 6 consecutive tetratricopeptid repeats (TPRs) while KDM6B lacks the TPR motif (Fig. 1) [35].

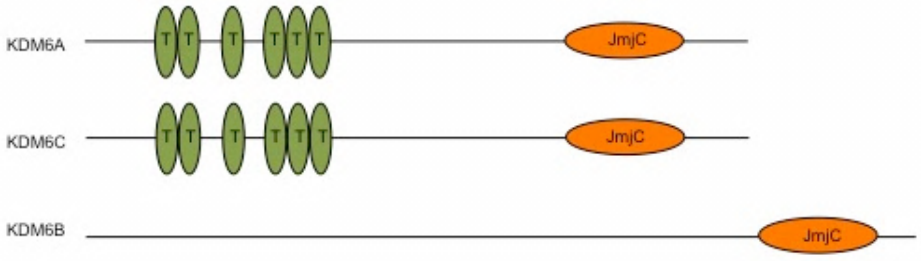

Fig. 1: Domain structure of KDM6A, KDM6C and KDM6B. Shown is the domain structure of KDM6A, KDM6C and KDM6B including the tetratricopeptid repeats of KDM6A and KDM6C and the Jumonji C domain which all three proteins contain. T: tetratricopeptid repeat; JmjC: Jumonji C domain (modified from Agger *et al.* [35]).

TPRs are protein-protein interaction modules and are found in multiple copies. KDM6A TPRs are required for the optimal demethylase activity of KDM6A on H3K27me1 but are dispensable for KDM6A activity on H3K27me3/2 [78].
The role of the KDM6C TPR domains remains elusive. Most proteins, which contain TPR motifs, appear in multiprotein complexes [81]. KDM6A and KDM6B are both components of the MLL/COMPASS like complex also known as the TrxG complex [75, 82].

1.3.1 Role of KDM6A and KDM6B in Undifferentiated ES Cells and During Differentiation

In the last decade many studies focused on the role of histone lysine demethylases particularly in ES cells and differentiating cells. However, the functional influence of KDM6A and KDM6B is not fully elucidated yet. Findings support evidence that KDM6A is not required for the proliferation of ES cells however, it contributes to the establishment of ectoderm and mesoderm *in vitro* [77, 83, 84]. Interestingly, this contribution is independent of the KDM6A enzymatic activity [77]. KDM6A homologues in zebra fish (KDM6A-1, KDM6A-2) have important roles in normal development [73, 77, 85]. In flies, KDM6A co-localizes with the elongating form of RNAPII, suggesting a role for H3K27 demethylation in transcriptional elongation [77, 86]. Further enzymatic activity of KDM6A is also required for hormone-mediated transcriptional regulation of apoptosis and autophagy genes during ecdysone-regulated programmed cell death of *Drosophila* salivary glands [87].

Female KDM6A KO embryos as well as some male KDM6A KO embryos show severe defects in the development of the notochord, hematopoietic and cardiac tissues and die in the uterus [72, 80, 83]. The survival of some male KDM6A KO embryos indicates that KDM6C may partially compensate for KDM6A. In addition, it was shown that KDM6A is a regulator for hematopoietic cell migration [83]. Adult female conditional KDM6A KO mice displayed myelodysplasia and splenic erythropoiesis whereas KDM6A KO males showed no phenotype [83].

The transcription factor HIF-1α leads to the induction of mouse and human KDM6B expression [88]. HIF-1α gets activated under hypoxia conditions and leads to the expression of genes, which are essential to maintain homeostasis. This might indicate a fundamental role for KDM6B during low oxygen concentrations being involved in regulating of cellular stress, DNA damage, DDR and finally cell death [88]. Knockdown (KD) of KDM6B in undifferentiated ES cells showed that KDM6B is required for the commitment of ES cells to the neural lineage [89]. KDM6B KO in mouse embryos causes perinatal lethality due to respiratory failure. A catalytic inactive KDM6B does not rescue this phenotype, which leads to the conclusion that KDM6B enzymatic activity is crucial for the establishment of respiratory function [89, 90].

A functional role of KDM6A and KDM6B was also shown during induced pluripotent stem (iPS) reprogramming of somatic to pluripotent stem cells [91, 92]. In this case KDM6A and KDM6B showed an antagonistic impact on reprogramming. While loss of KDM6A impeded reprogramming, the loss of KDM6B increased the reprogramming efficiency [91, 92]. Consequently, KDM6A is a positive and KDM6B a negative regulator of reprogramming.

Point mutations of KDM6A are found in patients who suffer from the Kabuki syndrome, a rare congenital anomaly syndrome [93]. Additionally KDM6A and KDM6B are frequent targets of somatic mutations in human cancers with high prevalence in multiple myeloma, breast cancer, prostate cancer, lung cancer and acute myeloid leukemia leading to the suggestion that H3K27 demethylases are tumour suppressor genes [94-98]. The database Cosmic (available at http://cancer.sanger.ac.uk/cosmic/gene/analysis) records for KDM6A around 257 diverse mutations found in multiple cancer types.

To elucidate the functional role of the H3K27me3-specific demethylases, Kruidenier and colleagues developed a small-molecule inhibitor (GSK-J4) specific for KDM6A and KDM6B [99]. The inhibition of both demethylases reduced lipopolysaccharide-induced proinflammatory cytokine production by human primary macrophages [99]. Thus far, a simultaneous inhibition of H3K27me3-specific demethylases in undifferentiated and differentiating ES cells was not analysed and might elucidate the functional role of KDM6A and KDM6B for maintaining ES cell pluripotency and upon ES cell differentiation.

1.3.2 The Interaction of KDM6A and KDM6B with Histone Modifying Complexes

KDM6A and KDM6B are components of the TrxG complex, which catalyse trimethylation of H3K4 and demethylase H3K27 (Fig. 2). The TrxG complex plays a fundamental role in pluripotent stem cells and is associated with transcriptional activation of genes involved in stem cell self-renewal [100]. In *Drosophila* the core protein of the TrxG complex is the eponymous trithorax (trx) protein itself while Set/MLL1-4 (Mixed-lineage leukemia) is the human homolog of the trx protein [101-103]. MLL is the methyltransferase of the TrxG complex and mediates the methylation of H3K4 [50]. The activating mark, H3K4me3, is frequently observed in promoter regions of pluripotent stem cells and is generally linked to transcriptional activation [104]. While the activating H3K4 mark is methylated, the repressive H3K27me3/2 mark is demethylated by KDM6A or KDM6B [35].

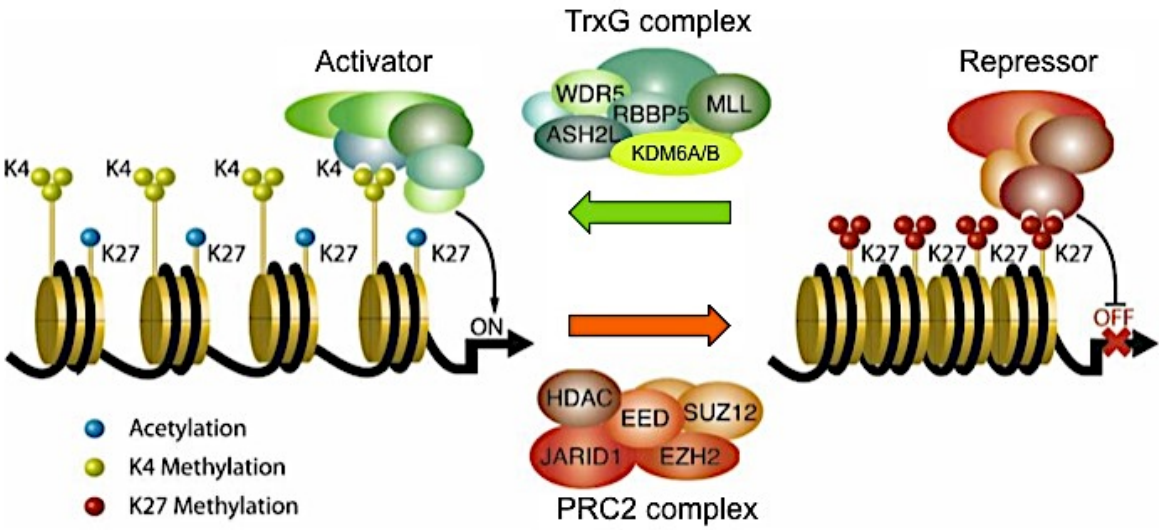

Fig. 2: Model for the involvement of demethylases/methyltransferases in transcriptional regulation. The TrxG complex and PRC2 complex contain both histone methyltransferase as well as histone demethylases in one and the same complex. The PRC2 complex (red) with the histone methyltransferase Ezh2 catalyses the repressive H3K27me3 mark, while Jarid1 removes the H3K4me3 mark resulting in gene silencing. The TrxG complex (green) activates transcription through the methylation of H3K4 catalysed by the histone methyltransferase MLL while KDM6A or KDM6B remove the repressive H3K27me3 mark (modified from Cloos *et al*. [50]).

Besides MLL and KDM6A and KDM6B, the TrxG complex contains further components *e.g.,* WDR5, ASH2L, RBBP5 and PTIP. The proteins WDR5, ASH2L and RBBP5 form the WAR sub-complex [105]. The WAR sub-complex and especially WDR5 interacts with H3K4me2 and mediates the transition of H3K4me2 to H3K4me3 [106]. PTIP is known to interact with 53BP1, a key regulator of DDR, and PTIP-deficiency results in genomic instability and DNA damage [107-109]. Interestingly, PTIP only occurs in the TrxG complex in association of KDM6A [50]. This indicates that KDM6A containing TrxG complexes might be involved in DDR and/or DNA repair [50]. Mutations of genes, which code for TrxG components, can also be linked to many diseases, *e.g.,* translocations of MLL were observed in human lymphoid and acute myeloid leukemia (AML) [110] while mutations of KDM6A and KDM6B could be associated with multiple myeloma [60].

The Jumonji-type histone demethylases are counter players of Polycomb group (PcG) proteins. PcG proteins are found in several families of multi-protein complexes, including the Polycomb Repressive Complexes 1 and 2 (PRC1 and PRC2) [111]. Both PRCs regulate developmental genes, *e.g.,* Homeobox (Hox) genes, and are essential for cell fate transitions [111, 112]. PRC2 mediates trimethylation on H3K27, a mark associated with gene silencing [113]. The PRC2 complex contains a H3K4-specific histone demethylase (Jarid1/2) as well as three core proteins (Ezh2, Suz12 and Eed (embryonic ectoderm development)) [114-116]. Eed binds with its WD40 domains to core regions of H3 or to histone tails of H3 carrying the K27me3 or K9me3 residues. This leads to the activation of Ezh2 [113]. Ezh2, a H3K27me-specfic histone methyltransferase, catalyses trimethylation of histone H3 at lysine 27 [114]. Finally, Suz12 interacts with Ezh2 and inhibits protein degradation of Ezh2 [117]. Suz12 is co-localized with H3K27 trimethylation at key development genes, as well as with highly conserved non-coding elements in ES cells [118]. Subsets of Suz12-bound and H3K27me3-enriched genes are co-occupied by Oct3/4, Sox2 and Nanog. These co-occupied genes are preferentially activated during ES cell differentiation, indicating that PRC2 poises differentiation-related genes for rapid gene activation during differentiation in pluripotent stem cells [21, 118]. Although PRC2 components are not necessarily required for the self-renewal of ES cells, they play an essential role for differentiation and lineage commitment [119-121]. Investigations showed that PRC2 murine KO ES cells, whether through KO of Eed,

Ezh2 or Suz12 lack global H3K27me3 level and result *in vivo* in early embryonic lethality [117, 119, 122-124]. This observation indicates that the activity of the PRC2 complex is dependent on all these three core components [125].

1.4 Goal of the Study

To analyse the functional consequences of a combined KDM6A and KDM6B inhibition in ES cells and during ES cell differentiation of wild type (WT) and Eed KO ES cells, which lack H3K27me3 marks, I used a specific small molecule inhibitor (GSK-J4). GSK-J4 inhibits the enzymatic activity of KDM6A and KDM6B while the molecular protein structure remains unaltered. In addition to the use of GSK-J4, I generated and employed KDM6A KO/KDM6B KD ES cells to investigate if the loss of KDM6A and KDM6B proteins also correlated with results received in response to GSK-J4. Finally, as an additional functional read out, I performed hematopoietic differentiation of murine bone marrow (BM) cells to investigate if colony forming potential is impaired under KDM6A and KDM6B inhibition.

2. Materials and Methods

2.1 Materials

2.1.1 Mice

Strain	Genetic background	Specific features	Source
DR4	129/Sv x C57BL6	four antibiotic resistance genes	Jackson Lab, Bar Harbor USA
CD1	129/Sv x C57BL6	wild type	Jackson Lab, Bar Harbor USA

2.1.2 Mouse ES cell lines

Name	Genetic background	Specific features	Source
R1	129/Sv X 129/Sv	wild type	AG Mueller, Wuerzburg D
J1	129/Sv X 129/Sv	wild type	Dr. Wutz, Zurich CH
Eed (J1)	129/Sv X 129/Sv	knockout of Eed	Dr. Wutz, Zurich CH
KDM6A KO (R1)	129/Sv X 129/Sv	knockout of KDM6A	Dr. Anastassiadis, Dresden D

2.1.3 Cell lines

Name	Genetic background	Specific features	Source
HeLa	human cervix	-	Dr. Schindler, Wuerzburg, D
293T	human embryonic kidney	contains SV40 T-antigen	ATCC, Wesel D

2.1.4 Cell culture media and supplements

Standard ES cell medium

Component	Concentration	Volume	Distributor
DMEM, high glucose		400 ml	Sigma Aldrich
FCS, pre-tested for ES cells	15%	75 ml	Gibco Invitrogen
Sodium pyruvate	1 mM	5 ml	PAA
Penicillin, Streptomycin	100 U/ml, 0.1 mg/ml	5 ml	PAA
L-glutamine	2 mM	5 ml	PAA
Non essential aminoacids	1x	5 ml	PAA
Beta-Mercaptoethanol	0.1 mM	3.5 µl in 5 ml Hepes	Sigma Aldrich, PAA
LIF-conditioned medium		500 µl	own production

Differentiation medium

Component	Concentration	Volume	Distributor
DMEM, high glucose		425 ml	Sigma Aldrich
FCS, pre-tested for EB differentiation	15%	50 ml	Gibco Invitrogen
Sodium pyruvate	1 mM	5 ml	PAA
Penicillin, Streptomycin	100 U/ml, 0.1 mg/ml	5 ml	PAA
L-glutamine	2 mM	5 ml	PAA
Non essential aminoacids	1x	5 ml	PAA
Beta-Mercaptoethanol	0.1 mM	3.5 µl in 5 ml Hepes	Sigma Aldrich, PAA

MEF medium

Component	Concentration	Volume	Distributor
DMEM, low glucose		435 ml	Sigma Aldrich
FCS, pre-tested for MEFs	10%	50 ml	Gibco Invitrogen
Sodium pyruvate	1 mM	5 ml	PAA
Penicillin, Streptomycin	100 U/ml, 0.1 mg/ml	5 ml	PAA
L-glutamine	2 mM	5 ml	PAA

Hematopoietic methylcellulose medium

Component	Concentration	Volume	Distributor
IMDM		22.56 ml	PAA
Basic methylcellulose	1%	40 ml	Stem Cell Technologies
FCS, pre-tested for EB differentiation	15%	15 ml	Gibco Invitrogen
Penicillin, Streptomycin	100 U/ml, 0.1 mg/ml	1 ml	PAA
L-glutamine	2 mM	1 ml	PAA
human IL-3	30 ng/ml	0.03 ml	PeproTech
human IL-6	30 ng/ml	0.03 ml	PeproTech
mouse SCF	150 ng/ml	0.15 ml	PeproTech
Epo	3 U/ml	0.06 ml	Prof. Sirén, Wuerzburg D
GM-CSF	50 ng/ml	0.05 ml	PeproTech
BIT9500 (1% BSA, 10 µg/ml Insulin, 200 µg/ml Transferrin	20%	20 ml	Stem Cell Technologies
MTG	4.5x10^-4 M	0.124 ml	Sigma Aldrich

HeLa/293T cell medium

Component	Concentration	Volume	Distributor
DMEM, low glucose		440 ml	Sigma Aldrich
FCS, pre-tested for MEFs	10%	50 ml	Gibco Invitrogen
Penicillin, Streptomycin	100 U/ml, 0.1 mg/ml	5 ml	PAA
L-glutamine	2 mM	5 ml	PAA

2.1.5 Antibodies

Primary antibodies

Specificity	Species	Distributor
H3	rabbit, polyclonal	Abcam
H3K27me3	rabbit, polyclonal	Diagenode
H3K27me2	rabbit, polyclonal	Abcam
γH2AX (Ser139)	mouse, monoclonal	Upstate
phospho-p53 (Ser15)	rabbit, polyclonal	Cell Signaling
p53	rabbit, polyclonal	Cell Signaling
Eed	rabbit, polyclonal	Millipore
KDM6B	rabbit, polyclonal	Abcam
GAPDH	mouse, monoclonal	Millipore
Ku80	rabbit, polyclonal	Cell Signaling
phospho-ATM/ATR substrates	rabbit, polyclonal	Cell Signaling
SSEA-1	mouse, monoclonal	Biolegend

Secondary antibodies

Specificity	Label	Distributor
rabbit	HRP	Thermo Scientific
mouse	HRP	Thermo Scientific
mouse	Cy5	Life Technologies
rabbit	Cy3	Chemicon
biotin (streptavidin)	PE-Cy7	BD

2.1.6 Primers

All qRT-PCR were performed using an annealing temperature of 60°C. Primers were obtained from Eurofins MWG Operon.

Gene	Sequence	Product size (bp)
KDM6A	GCTGGAACAGCTGGAAAGTC GAGTCAACTGTTGGCCCATT	111
KDM6A binding in Exon 3	CTGAAGGGAAAGTGGAGTCTG TCGACATAAAGCACCTCCTG	220
KDM6B	GGAAGCCACAGCTACAGGAG CCACCAGGAACCAGTCAAGT	296
UTY	ATAGTGTCCAGACAGCTTCA GAGGTAGGAATACGTAAGAA	232
KDM7A	GGAACTGGCACAGGCATGACTA CCTGAGTCCAAGGTCATCTAATTTA	221
Oct4	AGGCCCGGAAGAGAAAGCGAACTA TGGGGGCAGAGGAAAGGATACAGC	266
Sox2	GCGGAGTGGAAACTTTTGTCC CGGGAAGCGTGTACTTATCCTT	157
Nanog	TCTTCCTGGTCCCCACAGTTT GCAAGAATAGTTCTCGGGATGAA	100
HoxB1	GCCCCAACCTCTTTTCCCC GACAGGATACCCCGAGTTTTG	117
Neurog3	CCAAGAGCGAGTTGGCACT CGGGCCATAGAAGCTGTGG	236
Pou2F3	CTGGAACAGTAACGTCATCCTG AGTTCATTGCTGCTTTGGAGTT	120
Mdm4	TTCGGAACAAATTAGTCAGGTGC AGTGCATTACCTCTTTCATGGTG	104
Btg2	ATGAGCCACGGGAAGAGAAC GCCCTACTGAAAACCTTGAGTC	122
$p21^{CIP}$	CACAGCTCAGTGGACTGGAA ACCCTAGACCCACAATGCAG	111

Polk	AGCTCAAATTACCAGCCAGCA GGTTGTCCCTCATTTCCACAG	149
Trp53inp1	CTTCTCCTGTTTACCTGCATCTT TGATAGTGGTTAATCCACCTGCT	143
GAPDH	TGGAGAAACCTGCCAAGTATG TCATACCAGGAAATGAGCTTGA	199
RPL4	TTGGGTTGTATTCACTCTGCG CAGACCAGTGCTGAGTCTTGG	177
Ku 70	ATGTCAGAGTGGGAGTCCTAC TCGCTGCTTATGATCTTACTGGT	230
Ku 80	TGTCCAACGACAGGTATTTTCG AAGGGCATTATCAGTGCCATC	82
Eed	GCACAGAGATGAAGTTCTGAGTGCTG ATAAGACTCCTTAATTGCATTCATCATCCT	133

2.1.7 Plasmid vector

Plasmid vector	Drug resistance	Source
pMDL g/p RRE	ampicillin	addgene
pRSV-Rev	ampicillin	addgene
pMD2.G	ampicillin	addgene
pLKO.1 Mission Vector	ampicillin/puromycin	Sigma Aldrich

2.1.8 shRNA sequences

shRNA	Sequence	Target region
shRNA#1 (KDM6B_1)	CCTGTTCGTTACAAGTGAGAA	CDS
shRNA#2 (KDM6B_2)	CCTCGTCATCTCAGTTCTCTA	CDS
scrambled shRNA	CCTAAGGTTAAGTCGCCCTCG	non

2.1.9 Buffers and solutions

PBS

137 mM NaCl, 2.7 mM KCl, 10 mM Na_2HPO_4, 1.76 mM KH_2PO_4, pH 7.4

PBST

PBS, (0.1% Tween20)

10x TBS

0.2 M Tris Base, 1.5 M NaCl, pH 7.6

TBST

TBS, (0.1% Tween20)

Stacking gel buffer

0.5 M Tris-HCl, pH 6.8

Separation gel buffer

1.5 M Tris-HCl, pH 8.8

10x running buffer for Western blot

25 mM Tris-HCl pH 6.8, 192 mM Glycine, 0.1% (w/v) SDS

10x blotting buffer for Western blot

25 mM Tris-HCl pH 6.8, 192 mM Glycine, 20% (v/v) Methanol

FACS-buffer

PBS, 0.3% BSA, pH 7.4

Protein 2x loading buffer

0.5 M Tris-HCl pH 6.8, 0.4% SDS, 2% glycerol, 0.5% beta-mercaptoethanol and bromphenol blue

Trypsin

0.05% Trypsin, commercially purchased from PAA

Gelatin for cell culture

0.1% gelatin in PBS

Western blot stripping solution

0.2 mM NaOH

Gey's Solution

20% Stock A: 0.65 M NH_4Cl, 25 mM KCl, 0.87 mM Na_2HPO_4-12•H_2O, 0.88 mM KH_2PO_4, 27.8 mM Glucose, 0.14 mM Phenol red

5% Stock B: 2.07 mM $MgCl_2$-6•H_2O, 0.57 mM $MgSO_4$-7•H_2O, 3.06 mM $CaCl_2$

5% Stock C: 26.78 mM $NaHCO_3$, added 100% H_2O

2x HBS

0.14 mM NaCl, 5.1 mM KCl, 0.7 mM Na_2HPO_4, 0.02 mM Hepes, 5.55 mM Glucose, pH 7.05

$CaCl_2$ Solution

2.5 M $CaCl_2$

Permeabilization buffer

PBS, 0.1% TritonX-100

Blocking solution for IF

20% FCS in permeabilization buffer

DAPI

20 mg/ml in H_2O

Mowiol (mounting medium)

25 mg/ml in H_20

Fixation solution for cells

4% Paraformaldehyde in PBS

Sucrose solution for EB dehydration

20% Sucrose in PBS

2.1.10 Cell culture plastic

Cell culture plastic	Distributor
1.8 ml cryotubes	Thermo Scientific
6 cm TC plates	Greiner
10 cm TC plates	Greiner
3 cm Petri dish	SPL Life Sciences
10 cm Petri dish	Greiner
15 cm Petri dish	Greiner
75 m^2 TC flasks, red cap	Sarstedt
175 m^2 TC flasks, red cap	Sarstedt
24-well plates TC	Greiner
96-well plates TC	Greiner
96-well plates Petri dish	Greiner
15 ml tubes	Greiner
50 ml tubes	Greiner
70 µm cell strainer	BD
96-well plates for qRT-PCR	4titude
Neubauer chamber	Laboroptik
12 mm cover slips	Paul Marienfeld GmbH & Co. KG
45 µm PVDF filter	Greiner
superfrost microscope slides	Thermo Scientific

2.1.11 Technical device

Technical device	Distributor
FACS Canto I	BD
Roche Light Cycler 480	Roche
Cell culture microscope EVOS	AMG
Laser scanning microscope (LSM 780)	Zeiss
Qubit Fluorometer	Invitrogen
Chemidoc XRS low light imager	Biorad
Incubator Heracell 150	Thermo
Kryostat CM 1950	Leica
Faxitron CP-160	Faxitron X-Ray LLC

2.1.12 Commercial kits and reagents

Kit/Reagent	Distributor
First Strand cDNA Synthesis Kit	Fermentas
DNaseI	Fermentas
RNase	Fermentas
Alkaline Phosphatase Kit	Sigma Aldrich
Absolute SybrGreen Mix	Thermo Scientific
PeqGold RNAPure	PeqLab
RNeasy Mini Kit	Qiagen
AnnexinV-PE Apoptosis detection Kit	BD
DAPI	Sigma Aldrich
Mowiol (mounting medium)	Invitrogen
Nitrocellulose membrane	Schleicher & Schuell
Tissue-Tek	Sakura
PEG-it™ Virus Precipitation Solution	System Biosciences
Mitomycin C	Sigma Aldrich
RNase and DNase free water	Fermentas
DMSO	Sigma Aldrich

GSK-J5	Cayman
GSK-J4	Tocris
Chloroquin	Sigma Aldrich
Hexadimethrinebromid	Sigma Aldrich
Puromycin	Sigma Aldrich
Amersham ECL Select Western Blot Detection Reagent	GE Healthcare
Propidium Iodide	Sigma Aldrich
Bi-distilled water	Sigma Aldrich
ES-Cult M3120 (Basic methylcellulose)	Stemcell Technologies
Agarose	PeqLab
trypan blue	Sigma Aldrich

2.1.13 Software

Software	Distributor
ImageJ	NIH
FlowJo	Tree Star, Inc.
FACS DIVA	BD
Roche Light Cycler 480 Software	Roche Applied Science
ModFit LT ™	Verity software house
geNORM	Biogazelle
ZEN software	Zeiss
Micron	Evos AMG

2.2 Methods

2.2.1 Isolation of primary cells from mouse

Mouse Embryonic Fibroblast (MEF) isolation

MEFs were isolated from E13.5 mouse embryos of WT or DR4 mice. Pregnant mothers were sacrificed and embryos were carefully prepared by removal of extra embryonic tissue. The head and inner organs of the embryos were removed by a pair of forceps and the remaining embryonic tissue was minced by scalpel. The minced tissues of three embryos were transferred into 3 ml of trypsin solution and incubated (37°C, 45 min) in a water bath under constant agitation. The enzymatic reaction was stopped by adding 10 ml of MEF cell medium and the tissue was minced thorough pipetting. Finally, 10 µl of DNaseI (1 U/µl) was added. The embryonic suspension was centrifuged (90x g, 5 min) and the cell pellet was resuspended in MEF cell medium. Cells were plated at a density of 1/2 embryo per 10 cm TC plate. One day later attached MEFs were trypsinized and passed through a 70 µm cell strainer to obtain single cell solutions. One 10 cm TC plate was frozen in three cryotubes and marked as passage 0.

Bone Marrow isolation

Male C57BL6 mice at an age of 8 to 12 weeks were sacrificed, femur and tibia bones were isolated and the BM was flushed out with 0.3% BSA in PBS by using a syringe. To obtain a single cell suspension the cell solution was passed through a 70 µm cell strainer, centrifuged (1700 rpm, RT, 5 min). Erythrocytes were depleted by incubation in hypotonic Gey's solution (4°C, 5 min) and the BM cells were subsequently collected in a phase of FCS by centrifugation (1700 rpm, RT, 5 min).

2.2.2 Cell Culture

All cells were cultured at 37°C with 5% CO_2 in a humidified atmosphere. ES cells were frozen in FCS containing 10% DMSO while MEFs, 293T cells and HeLas were frozen in cell medium containing 10% DMSO. All cells were frozen at -80°C.

MEFs

MEFs were either used directly upon isolation or thawed from frozen stocks. Cells were maintained in TC flasks (T75 or T175) with MEF cell medium and split every other day. Therefore cells were washed once with PBS and incubated with 1.5 or 3 ml of trypsin (37°C, 3-5 min). The reaction was stopped by addition of 10 ml MEF cell medium. After centrifugation (90x g, 5 min) cells were passaged in a ratio of 1:2. For mitotic inactivation, confluent MEF cultures were treated with Mitomycin C (MitC) (10 µg/ml) (37°C, 2 h), washed 2x with PBS and trypsin was added. The enzymatic reaction was stopped and cells were counted. Mitotic inactivated MEFs were plated at a density of ≥0.4x10^6 cells per 6 cm TC plate and were used as feeder cells for subsequent ES cell culture.

ES cells

ES cells were thawed and cultivated on a monolayer of MitC inactivated MEFs in 6 cm TC plates in the presence of ES cell medium. Medium was replaced every day and cells were passaged every other day. For passaging the medium was removed and cells were washed 2x with PBS followed by incubation with 0.5 ml trypsin (37°C, 5 min). Trypsin reaction was stopped by adding 5 ml of ES cell medium and cells were dissociated by pipetting. After centrifugation (90x g, 5 min) the pellet was resuspended in ES cell medium and 0.5x10^6 cells were given in ES cell medium to a new culture dish onto MEFs.

To separate ES cells from MEFs gelatin coated plates were used. Therefore 10 ml of a 0.1% gelatin solution was given on a 10 cm TC plate which was incubated for at least 30 min at 37°C. After incubation time gelatin solution was removed and the heterogeneous cell suspension of one 6 cm TC plate (comprising ES cells and MEFs) was given on the 10 cm plate. Incubation (37°C, 5% CO_2, 45 min) followed. This allowed MEFs to attach to the bottom of the dish while ES cells only loosely adhere and dead cells as well as cell clusters remain in suspension. Single cell

suspension of ES cells were obtained by removing the suspension phase and with PBS the loosely adhered ES cell fraction where washed off. Life cell numbers were determined by trypan blue staining and counted in a Neubauer chamber.

ES cell differentiation

ES cell differentiation is performed by culturing ES cells in non-attached dishes in suspension or as hanging drops on the lid of Petri dishes.

For differentiation in suspension, 1-2x10^6 feeder-depleted ES cells were cultured in a 10 cm Petri dish in 10 ml EB medium.

For limited dilution experiments 2-4000 ES cells were cultured in 100 µl EB medium for each well of a non-attached 96-well plate.

For hanging drop differentiation 0.33x10^5 ES cells were resuspended in 1 ml of EB medium. Drops (120 for each plate) with the volume of 30 µl each (1.000 ES cells per drop) were transferred to the lid of a 15 cm Petri dish. To prevent dehydration of hanging drops 10 ml of PBS was given on the bottom of the Petri dish. After 2 days EBs from one 15 cm Petri dish were transferred to a 10 cm Petri dish by washing hanging drops off the lid with 10 ml EB medium.

EB medium was changed every other day. For harvesting, EBs were transferred to Falcon tubes and allowed to sediment. For preparation of single cell suspension EB medium was replaced by 1 ml trypsin followed by incubation (37°C, 3 min) in a water bath. Trypsin reaction was stopped by adding 5 ml of EB medium and cells were dissociated by pipetting. Life cell numbers were determined by trypan blue staining and counted in a Neubauer chamber.

HeLa/293T cell culture

HeLa and 293T cells were thawed from frozen stocks and cultured in appropriate medium in T75 tissue culture flasks. Cells were passaged every other day. For passaging cells the medium was removed and cells were washed once with PBS followed by incubation (37°C, 5 min) with 1.5 ml trypsin. Trypsin reaction was stopped by adding 10 ml of medium and cells were dissociated by pipetting. After centrifugation (90x g, 5 min) the pellet was resuspended in medium and 1x10^6 cells were given to a new culture flask.

Treatment of cells with GSK-J4 and GSK-J5

GSK-J4 and GSK-J5 were dissolved in DMSO and frozen as aliquot stocks at -20°C. Stocks were not refrozen. Both compounds were added to ES cell or EB medium at a concentration of 1.9 µM. The inhibitor concentration was selected based on increased methylation level of H3K27me3 without loss of cell viability in ES cells. After addition of GSK-J4 or GSK-J5 cells were cultured on the same schedule described above.

CPD and PD determination

For analyses of Cumulative Population Doublings (CPD) feeder-depleted ES cells were seeded onto MitC inactivated MEFs at a density of 0.5x10^6 in 6 cm TC plates. After 2 days of culture feeder-depleted ES cells were counted by trypan blue staining. Subsequently 0.5x10^6 ES cells were reseeded and cells were sub-cultured for a total of three passages. The Population Doubling (PD) level at each passage was determined according to the following equation: $x = \log10\ [\log10(N_1) - \log10(N_H)]$ where N_1 = inoculum number, N_H = cell harvest number and x = PD [126]. New PD level values were added to previous values to calculate CPD values.

ES cell colony formation assay

To analyse if ES cells keep the potential to form pluripotent colonies 5x10^3 feeder depleted ES cells were seeded on a MitC inactivated MEF feeder layer in a 24-well TC plate. After 2 days the colonies were fixed with fixation solution and the activity of their Alkaline Phosphatase (AP) was investigated using the AP kit following manufacturers instructions. Only colonies, which were positive for AP indicated by red colour, were enumerated by light microscopy.

Hematopoietic colony formation assay

Freshly isolated BM cells were plated in a 3 cm Petri dish at a density of 5×10^4 cells in 1 ml of blast colony forming cell (BL-CFC) methylcellulose medium containing a cocktail of growth factors (see chapter 2.1.4). Cells were maintained at 37°C in a humidified 5% CO_2 atmosphere. After 4 days BL-CFCs were counted.

Lentiviral transduction

One day before $CaCl_2$-transfection was performed 1.4x10^6 293T cells were plated into a 10 cm TC dish in 10 ml 293T cell medium. The next day medium was removed and replaced by 293T cell medium containing 4.38 µg/ml Chloroquin. Cells were incubated for at least 30 min at 37°C and 5% CO_2. Plasmids [(transfer vector 20 µg (Mission Vectors), packaging plasmid (pMDL g/p RRE – 10 µg, pRSV-Rev – 5 µg) and envelope plasmid (pMD2.G 6 µg)] were added to a total of 500 µl H_2O. 500 µl of a 2x HBS Puffer and 50 µl of a 2.5 M $CaCl_2$ solution was added. The solution was incubated (RT, 25 min) and added drop wise to 293T cells. Cells were incubated (37°C, 5% CO_2, 6-8 h) before the medium was replaced by 5 ml 293T cell medium. After two days the supernatant, containing lentiviral particles, was collected and centrifuged (3000x g, RT, 15 min). Subsequently the supernatant was filtered through a 0.45 µm PVDF filter and 1 volume of cold PEG-*it* ™Virus Precipitation Solution was added. The suspension was incubated (4°C, ≥12 h). The following day ES cells were seeded, at least 5 hours prior first lentiviral transduction, onto MEFs. The virus containing supernatant was centrifuged (1500x g, 4°C, 30 min) and the pellet was resuspended in ES cell medium containing hexadimethrine bromide (8 µg/ml). The ES cell medium of seeded ES cells was replaced by medium containing the lentiviral particles/hexadimethrine bromide followed by a centrifugation step (2300 rpm, RT, 90 min). After the centrifugation cells were incubated (37°C, 5% CO_2). The next day a second transduction was performed. Two days after the second transduction ES cells were selected with selection medium containing Puromycin (1 µg/ml). Before experiment started cells were kept under selection for at least 4 days and throughout experiment.

2.2.3 Molecular biology

RNA isolation

Total RNA was extracted using RNeasy Mini or peqGOLD RNAPure kits following manufacturers instructions. Concentration was measured by using a Qubit fluorometer. As quality control 1 µg of total RNA was loaded on a 1.2% agarose gel containing 1.8 ml 37% formaldehyd. Intact RNA showed sharp and clear bands of 28S and 18S rRNA and was used for cDNA synthesis.

cDNA synthesis

cDNAs were synthesized using the First Strand cDNA Synthesis Kit. Briefly, 1 µg of total RNA was used. Prior to cDNA synthesis genomic DNA was digested by adding DNaseI (1 U/µl) (37°C, 30 min). The reaction was stopped by the addition of 50 mM EDTA followed by a heat inactivation (65°C, 10 min). Random hexamer primers were allowed to anneal to RNA (65°C, 5 min) followed by an incubation on ice for 1 min. In the last step of cDNA synthesis 5 mM dNTPs, RiboLock RNase Inhibitor (40 U/µl), M-MuLV reverse transcriptase (20 U/µl) and 5x reaction buffers were added. The probes were incubated (37°C, 1 h) and to inactivate enzymes a heat inactivation (70°C, 5 min) followed.

Quantitative Real Time-PCR (qRT-PCR)

For gene expression analyses 1 µl of cDNA was mixed with 10 µl 2x SybrGreen Mix, 5 µl of 10 pM primers and 4 µl H_2O. All reactions were carried out as duplicates or triplicates in a Roche Light Cycler 480 II using the following conditions: initial denaturation for 15 min at 95°C, followed by cycles of 10 s at 95°C, 20 s at 60°C, and 30 s at 72°C. CT values were normalized to two housekeeper genes (GAPDH and RPL4) which were pre-selected based on their stable expression using geNorm software.

Global gene expression analysis (Microarray)

For global gene expression analysis total RNA was extracted using RNeasy Mini Kit following manufacturers instructions. RNA was handed over to the Core Unit Systemmedizin, which performed further analysis.

Western blot

Single cell suspensions were washed twice with PBS prior lysis in 2x loading buffer. Lysates were adjusted to 1x10^6 cells/125 µl, sheared by passing through a 21 gauge needle (at least 10 times) and heated (95°C, 5 min). Proteins were separated by SDS PAGE in 14% SDS gels and blotted onto nitrocellulose membranes. Membranes were blocked in PBS, 0.05% Tween20, 5% milk powder (RT, 30 min) followed by overnight incubation with primary antibodies. The next day membranes were washed 3x with PBST followed by incubation with secondary antibodies (RT, 1 h). After 3x washes in PBST membranes were covered with Amersham ECL Select Western Blot Detection Reagent (RT, 5 min). Chemiluminescence was detected on a Chemidoc XRS low light imager. If phospho-specific antibodies were used PBST was replaced by TBST. Intensity of protein bands was determined using ImageJ software. Membranes were stripped from antibodies using a stripping solution (RT, 20 min).

2.2.4 Flow cytometry

All flow cytometric analyses were performed on a BD FACS Flow Cytometer using FACS Diva and FlowJo software.

Analysis of cell cycle phase distribution

For analyses of cell cycle phase distribution propidium iodide (PI) stainings of single cell suspensions were performed. Cells were washed 2x with cold PBS, permeabilized with 70% EtOH and incubated for a minimum of 30 min at -20°C. After 2x washing steps with PBS cells were incubated (37°C, 30 min) in 200 µl PBS with RNase (10 µg/µl) and PI (10 µg/µl) prior FACS analyses. Cell cycle phase distribution was modelled with ModFit software.

Determination of SSEA-1 positive cell frequencies

Single cell suspensions of feeder-depleted ES cells were washed 2x with ice cold FACS-buffer and stained with anti-mouse SSEA-1 (4°C, 45 min). Cells were washed 2x with PBS and incubated with a secondary PE-Cy7-antibody (4°C, 45 min). Subsequently cells were washed 2x with PBS and measurements were performed.

Frequencies of apoptotic cells

Frequencies of apoptotic cells were analysed by using the Apoptosis detection kit. 2x10^5 feeder-depleted ES cells or EBs were washed once in 1x binding buffer and were incubated in the dark (RT, 15 min) with 5 µl 7-AAD and 5 µl AnnexinV-PE in 100 µl 1x binding buffer. Measurements were performed immediately.

2.2.5 Microscopy

All microscopic inspections were carried out on a inverted confocal laser scanning microscope (LSM780, Zeiss).

Immunofluorescence

For preparation of fixed ES cells, cells were grown on MitC inactivated MEFs on 12 mm cover slips for 2 days. Subsequently ES cells were fixed with 4% PFA (RT, 10 min) followed by 3x washing steps with PBS. For preparation of tissue sections EBs were transferred to Falcon tubes and allowed to sediment. After washing EBs 2x with PBS they were fixed with 4% PFA (4°C, 3 h) and dehydrated overnight in a 20% sucrose solution at 4°C. For exposure of ES cells or EBs to ionizing radiation (IR) cells were irradiated in ES cell medium or EB medium and immediately after irradiation fixed with 4% PFA as described above. Irradiation was carried out in a Faxitron CP-160 X-ray radiation cabinet (160 kV, 6.3 mA, 0.71 Gray/min, filter: 0.5 mm Cu). EBs were embedded in Tissue-Tek, 5 µm sections were mounted on superfrost microscope slides. Fixed ES cells or EB sections were permeabilized (0.1% TritonX-100 in PBS) for 30 min at RT followed by incubation in blocking solution (20% FCS, 0.1% Triton X-100 in PBS) for 30 min. Subsequently samples were incubated over night at 4°C with primary antibodies diluted in blocking solution. The following day samples were washed 3x times with PBS before incubation with the secondary antibody (RT, 1 h) diluted in blocking solution. Samples were subsequently washed 3x with PBS. DAPI (5 µg/ml) was added in the last washing step followed by mounting in Mowiol. The settings of GSK-J5 and GSK-J4 images or 6 Gy irradiated and control images were identical. For counting foci numbers per nucleus foci images of approximately 100 - 650 cells in total were analysed for average number of γH2AX foci per cell. For comparison between WT and Eed KO EBs, a constant exposure time for γH2AX was used.

3. Results

3.1 Inhibition of KDM6A and KDM6B enzymatic activity is incompatible with ES cell differentiation

3.1.1 Cell survival and global H3K27me3 levels in KDM6A and KDM6B inhibitor-treated ES cells

To investigate the role of the combined KDM6A and KDM6B demethylase activities in undifferentiated and differentiating ES cells a cell permeable small-molecule inhibitor was employed [99]. The inhibitor GSK-J4 is selective for the H3K27me3/2-specific demethylases KDM6A and KDM6B. GSK-J5, an inactive regio-isomer of GSK-J4 served as a control [99]. Both compounds were resolved in DMSO, hence DMSO served as an additional control. Dose finding experiments were performed with murine ES cells to identify optimal treatment conditions with high cell survival and maximum demethylase inhibition (corresponding to high H3K27me3 levels). Three different dilutions of the KDM6A and KDM6B inhibitor (GSK-J4) were tested. Best ES cell survival was observed at a concentration of 1.88 µM (Fig. 3A). Compared to controls all three dilutions showed globally increased H3K27me3 levels (Fig. 3B). The concentration of 1.88 µM showed the highest H3K27me3 level.
Since the GSK-J4 concentration of 1.88 µM showed the best cell survival and additionally the most globally increased H3K27me3 levels GSK-J4 was used for further experiments at a concentration of 1.88 µM.

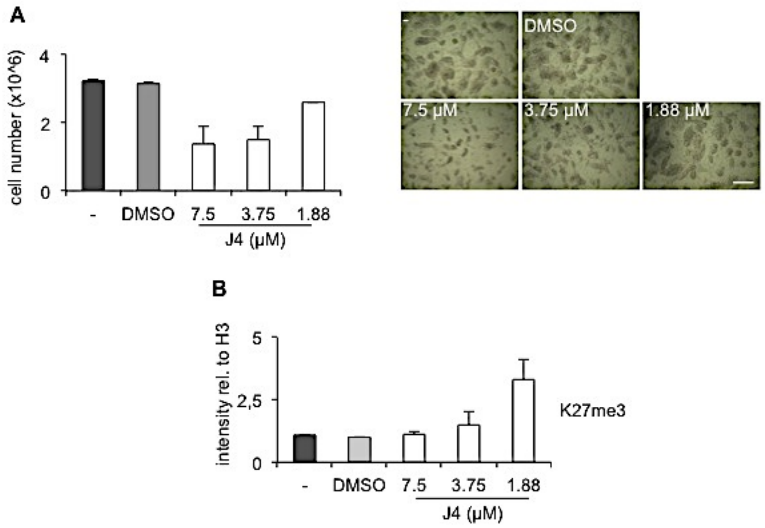

Fig. 3: Cell survival and global H3K27me3 levels in inhibitor-treated ES cells. A) Cell number of undifferentiated ES cells (0.5x10^6 cells seeded at day 0) grown on MEFs for 2 days in the presence of ES cell medium (-), DMSO (vehicle) or dilutions of GSK-J4 (J4, KDM6A/B inhibitor) (left). Micrographs of undifferentiated ES cells grown on MEFs for 2 days in the presence of ES cell medium (-), DMSO or dilutions of GSK-J4 (right). Scale bar = 100 µm. B) Diagram shows global H3K27me3 levels relative to H3 as determined by densitometric analyses of Western blot analyses of undifferentiated ES cells cultured in the presence of ES cell medium (-), DMSO or GSK-J4 for 2 days. A), B) Shown are means of two independent experiments. Error bars represent SEM. All experiments were performed with R1 ES cells.

3.1.2 GSK-J4 treatment leads to increased H3K27me3 levels in undifferentiated and differentiating ES cells and is incompatible with ES cell differentiation

As a next step, the consequences of inhibitor treatment on global H3K27me3/2 levels and cell survival in undifferentiated and differentiating ES cells were analysed.
As shown in Fig. 4A, treatment of undifferentiated and differentiating ES cells with GSK-J4 led to a two- to three-fold increase of global H3K27me3 levels while dimethyl levels were unaffected in undifferentiated and differentiating ES cells. The presence of GSK-J4 showed no effect on cell survival in undifferentiated ES cells (Fig. 4B). Surprisingly, ES cell differentiation in the presence of GSK-J4 led to a reduced cellularity of EBs (Fig. 4C).

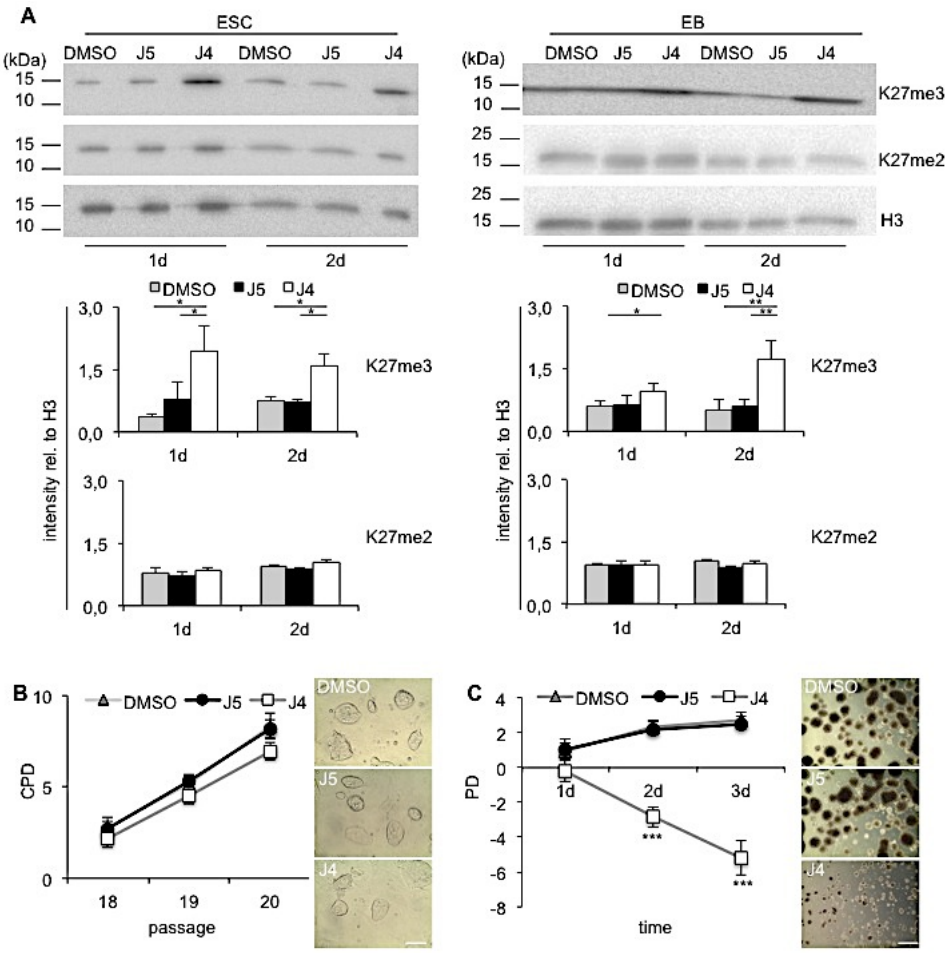

Fig. 4: Inhibition of KDM6A and KDM6B demethylase activity with GSK-J4 is incompatible with EB formation. A) (top) Western blot analyses of undifferentiated ES cells (ESCs, left) and embryoid bodies (EBs, right) cultured in the presence of DMSO, GSK-J5 (J5, control compound) or GSK-J4 for the indicated periods were probed with antibodies specific for H3K27me3, H3K27me2 or H3 (loading control). Graphs (bottom) show H3K27me3 and H3K27me2 levels relative to H3 as determined by densitometric analyses. B) Cumulative population doublings (CPD) of undifferentiated ES cells were cultured for three passages in the presence of DMSO, GSK-J5 or GSK-J4 (left) and micrographs of undifferentiated ES cells grown on MEFs for 2 days in the presence of DMSO, GSK-J5 and GSK-J4 (right). Scale bar = 100 µm. C) Population doublings (PD) of differentiating ES cells in suspension cultures (2x10^6 cells seeded at day 0) cultured for up to 3 days in the presence of DMSO, GSK-J5 or GSK-J4 (left) and micrographs of EB cultures at day 3 (right). Scale bar = 500 µm, d = days. A) - C) Shown are means of three independent experiments. Error bars represent SEM. *: p≤ 0.05; **: p≤ 0.01; ***: p≤ 0.001. All experiments were performed with R1 ES cells.

These results suggest that chemical inhibition of KDM6A and KDM6B led to increase H3K27me3 levels in ES cells and EBs while H3K27me2 levels were not affected. Further, the inhibition of KDM6A and KDM6B showed no effect on ES cell viability and morphology while treated ES cells did not generate EBs.

3.1.3 Expression analyses of KDM family members during KDM6A and KDM6B inhibition

To assess whether inhibitor treatment, which results in elevated H3K27me3 levels, affects expression levels of KDMs relative expression analyses of K27-specific KDMs in undifferentiated and differentiating ES cells +/- GSK-J4 were performed.
Treatment with GSK-J4 showed no altered expression levels of KDM6A, KDM6B or KDM6C and KDM7A in undifferentiated ES cells. Interestingly, in differentiating ES cells under GSK-J4 treatment increased expression levels of KDM6A, KDM6B or KDM6C and KDM7A were detected (Fig. 5).
These data indicate that elevated H3K27me3 levels upon GSK-J4 treatment did not cause a reduction of K27-specific KDMs in undifferentiated and differentiating ES cells.

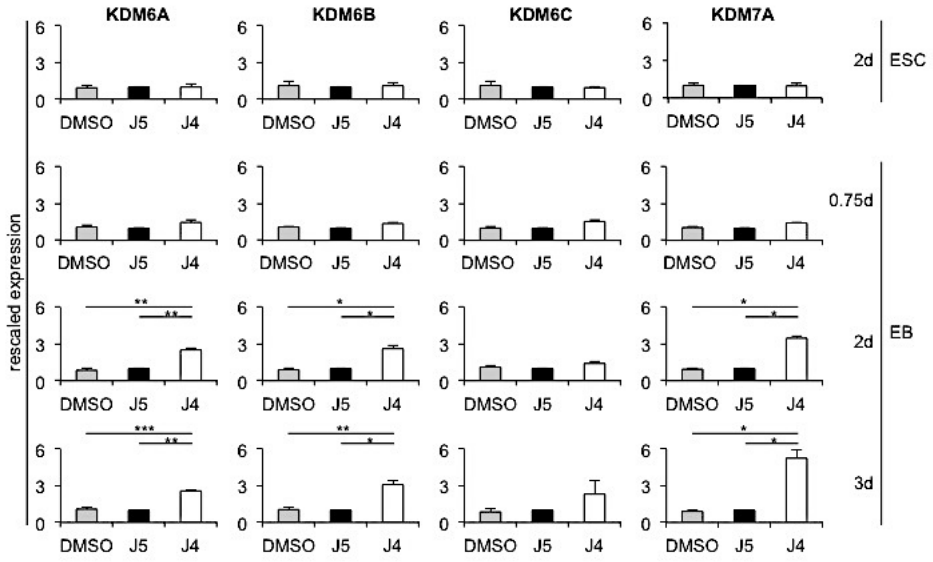

Fig. 5: Expression analyses of KDM family members during KDM6A and KDM6B inhibition. Undifferentiated or differentiating ES cells were treated for the indicated periods with DMSO, GSK-J5 or GSK-J4 before RNAs were prepared and qRT-PCRs were performed. Expression levels were normalized to GAPDH and RPL4. Shown are means of three independent experiments. Error bars represent SEM. *: p≤ 0.05; **: p≤ 0.01 ***: p≤ 0.001. All experiments were performed with R1 ES cells.

3.1.4 GSK-J4 treatment of undifferentiated ES cells has no effect on colony formation, expression of pluripotency factors or SSEA-1 positive cell frequencies

The next experiments were performed to determine if GSK-J4 treatment affects ES cell pluripotency. As shown in Fig. 6A colony formation potential of GSK-J4-treated ES cells, determined by AP positive colonies, remained unaltered compared to control ES cells. Furthermore, DMSO-, GSK-J5- or GSK-J4-treated ES cells showed ES cell-typical morphology (Fig. 6A, right).

Expression analyses of core pluripotency factors, Oct4, Sox2 and Nanog were analysed by qRT-PCR. These analyses showed no altered expression in ES cells incubated either with DMSO, GSK-J5 or GSK-J4 (Fig. 6B).

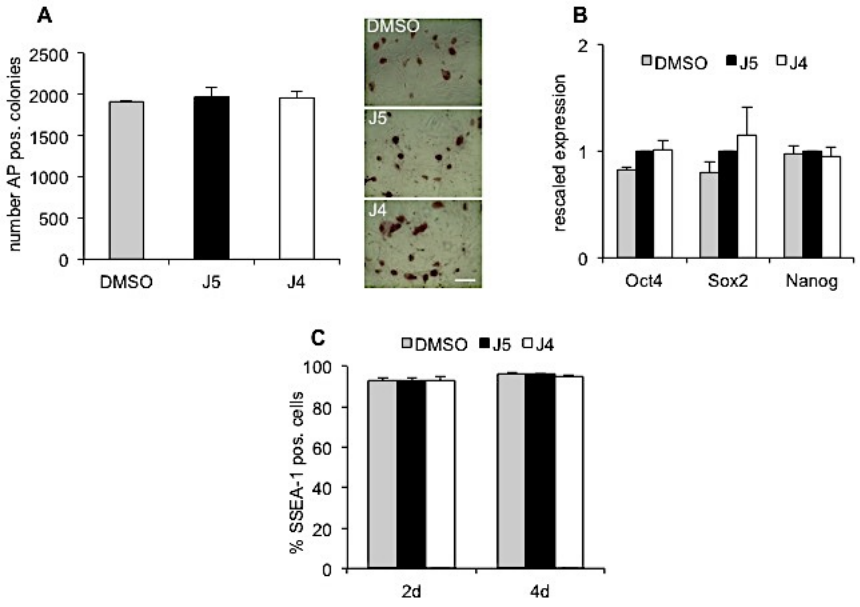

Fig. 6: GSK-J4 treatment of undifferentiated ES cells has no effect on colony formation, expression of pluripotency factors or SSEA-1 positive frequencies. A) 5000 undifferentiated ES cells were plated into 24-well plates and cultured in the presence of DMSO, GSK-J5 or GSK-J4 for 2 days and subjected to AP staining. Shown are numbers of AP-positive colonies (left) and representative micrographs of AP-positive undifferentiated ES cell colonies indicated by red colour (right). Scale bar = 100 µm. B) Gene expression of Oct4, Sox2 and Nanog in undifferentiated ES cells which were cultured for 2 days under ES cell conditions with DMSO, GSK-J5 or GSK-J4 before qRT-PCR was performed. Expression levels were normalized to GAPDH and RPL4. C) Levels of SSEA-1 positive undifferentiated ES cells cultured for 2 or 4 days in the presence of DMSO, GSK-J5 or GSK-J4. A) - C) Shown are means of three independent experiments. Error bars represent SEM. All experiments were performed with R1 ES cells.

Finally SSEA-1 stainings were performed to investigate if GSK-J4 treatment changed SSEA-1 levels and frequencies of SSEA1 positive cells. ES cells cultivated in the presence of GSK-J4 had similar levels and frequencies of SSEA1 positive cells compared to control cultures (Fig. 6C).
In conclusion GSK-J4 treatment of ES cells did not alter colony forming potential, expression of core pluripotency factors or SSEA-1 levels and frequencies. Based on these experiments the pluripotency of GSK-J-4 treated ES cells remained unaltered.

3.1.5 Inhibition of KDM6A and KDM6B enzymatic activity leads to cell death and cell cycle arrest in differentiating ES cells

As depicted in Fig. 4C differentiation of ES cells under KDM6A and KDM6B inhibition was disrupted with a significant loss of cellularity. To address the question whether the reduced cellularity is associated with an increased rate of apoptotic cells and altered cell cycle phase distribution apoptosis and PI stainings were performed. In the presence of GSK-J4 undifferentiated ES cells showed no altered frequency of apoptotic cells (Fig. 7A, left) in contrast to 2 day-old differentiated ES cells. Those showed a two- to three-fold increased level of apoptotic cells (Fig. 7A, right). The increased frequency of apoptotic cells goes along with a G0/G1-phase arrest in GSK-J4 treated EBs (Fig. 7B, right) while ES cells showed no alteration in cell cycle phase distribution (Fig. 7B, left).
In summary, inhibition of KDM6A and KDM6B enzymatic activity increased the rate of apoptotic cells and led to a G0/G1-phase arrest in differentiating ES cells while it did not affect undifferentiated ES cells.

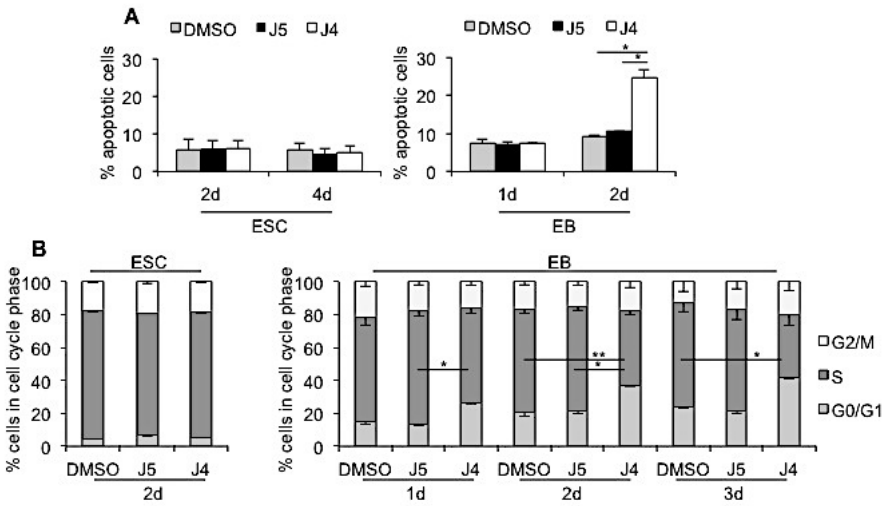

Fig. 7: Inhibition of KDM6A and KDM6B demethylase activity induces cell death and cell cycle arrest in differentiating ES cells. A) Fraction of apoptotic cells in response to inhibitor treatment. Undifferentiated and differentiating ES cells were cultured in the presence of DMSO, GSK-J5 or GSK-J4 for 2 or 4 days (ES cells) and 1 or 2 days (EBs) before single cell suspensions were analyzed by combined 7-AAD/Annexin V staining. B) Relative cell cycle phase distribution of ES cells (2 days) or EBs (1, 2 or 3 days). After incubation with DMSO, GSK-J5 or GSK-J4 cells were subjected to PI/FACS analyses for quantification of percentages of cells in G0/G1-, S- or G2/M-phase. A), B) Shown are means of three independent experiments. Error bars represent SEM. d = days. *: p≤ 0.05; **: p≤ 0.01. All experiments were performed with R1 ES cells.

3.1.6 GSK-J4 pre-treatment of ES cells does not inhibit ES cell differentiation

Next, I asked whether undifferentiated ES cells, cultured in the presence of GSK-J4, had the potential to differentiate after GSK-J4 removal. To this end limited dilution experiments with differentiating ES cells were performed.

GSK-J4 pre-treated ES cells were able to differentiate when GSK-J4 was removed upon differentiation while GSK-J4 pre-treated ES cells differentiated in the presence of GSK-J4 showed a strongly reduced EB formation (Fig. 8, right).

These data suggest that GSK-J4 pre-treated ES cells were able to differentiate when GSK-J4 was removed.

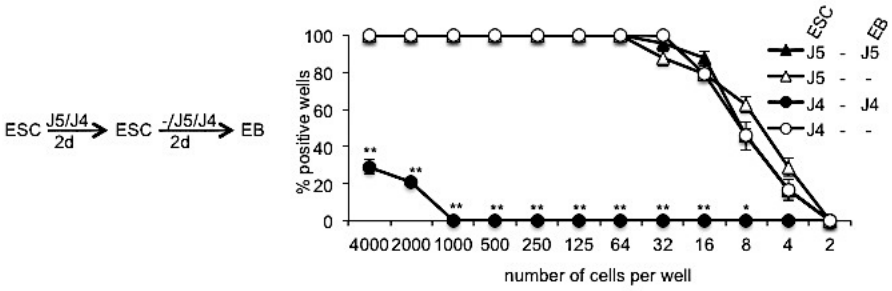

Fig. 8: GSK-J4 pre-treatment of ES cells does not inhibit ES cell differentiation. Experimental strategy (left). Undifferentiated ES cells were cultured in the presence of GSK-J5 or GSK-J4 for 2 days under ES cell conditions followed by a limited dilution experiment. Therefore undifferentiated ES cells were seeded with indicated cell numbers in a well of non-attach 96-well plate and were incubated for 2 days in differentiation medium in the presence of GSK-J5, GSK-J4 or differentiation medium only (-). Two days after differentiation wells with formed EBs were counted as positive wells. Shown are means of three independent experiments. Error bars represent SEM. *: p≤ 0.05; **: p≤ 0.01. Experiments were performed with R1 ES cells.

3.2 GSK-J4 treatment of differentiating ES cells leads to DNA Damage and DNA Damage Response (DDR)

3.2.1 Transcriptome analyses of differentiating ES cells

In order to investigate the mechanisms underlying the GSK-J4-induced effects on differentiating ES cells whole transcriptome analyses was performed. An early time point of differentiation was used to avoid apoptotic signatures.

Whole transcriptome analyses revealed that in total 303 genes were differentially expressed (Table 2) when ES cells were differentiated in the presence of GSK-J4 compared to GSK-J5 or DMSO treated cells (Fig. 9A). Surprisingly, under GSK-J4 treatment more genes were up-regulated (228) than down-regulated (75). Gene ontology (GO) analysis revealed that a large fraction of responsive genes were categorized as *e.g.,* ‘biological regulation’ (140), ‘metabolic process’ (137), ‘response to stimulus’ (109), ‘developmental process’ (77) or ‘cell communication’ (70). Many up-regulated genes belong to categories ‘death’ (44) and ‘cell proliferation’ (33) and gave strong indications for an activated DDR (Fig. 9B).

To confirm results from the global transcriptome analyses qRT-PCR analyses for a limited set of genes were performed (Fig. 9C). Of particular interest were down-regulated lineage markers (*e.g.,* Hox1 and Neurog3) and up-regulated genes with a role in DDR (*e.g.,* Btg2, Mdm4, $p21^{CIP}$, Polk and Trp53inp1) whose aberrant expression might relate to the incompatible ES cell differentiation.

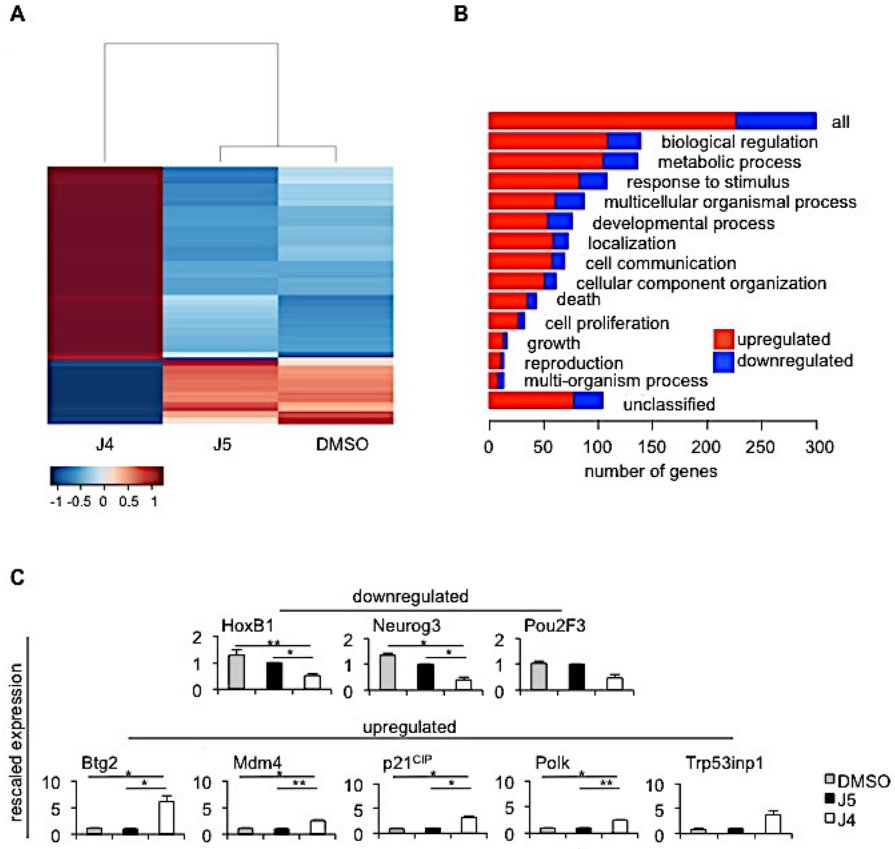

Fig. 9: GSK-J4 treatment induces differential expression of 303 genes in differentiating ES cells. A) Heat map of genes, which were differentially expressed in ES cells differentiated for 0.75 day in the presence of DMSO, GSK-J5 or GSK-J4. The hierarchical clustering dendrogram (top) indicates the relatedness in total gene expression. B) Differentially expressed genes from the transcriptome analyses were categorizes in GO terms using GO-slim software. The abscissa of the bar plot shows the number of genes within each GO category. C) Differentiating ES cells were cultured for 0.75 day in the presence of DMSO, GSK-J5 or GSK-J4 before RNAs were prepared and qRT-PCRs of genes, which were identified as differentially expressed under GSK-J4 treatment in the transcriptome analyses, were performed. Expression levels were normalized to GAPDH and RPL4. Shown are means of three independent experiments. Error bars represent SEM. *: p≤ 0.05; **: p≤ 0.01. A), B) In collaboration with Dr. Heike Weber from the Core Unit Systems Medicine, Wuerzburg transcriptome analyses were performed. A) - C) All experiments were performed with R1 ES cells.

In summary, transcriptome analyses showed that under GSK-J4 treatment particularly genes, which are associated with DDR, were upregulated. Subsequently, the focus was set on the role of KDM6A and KDM6B in DNA damage and DDR.

3.2.2 Inhibition of KDM6A and KDM6B induces DNA damage signalling in differentiating ES cells

The kinases Ataxia telangiectasia mutated (ATM) and ataxia telangiectasia and Rad3-related (ATR) activate more than 700 downstream targets through phosphorylation in response to DNA damage and are therefore central components to the DDR cascade [127]. To assess if GSK-J4 treatment in differentiating ES cells results in increased activation of DNA damage-associated factors downstream targets of ATM/ATR were analysed.

ES cells differentiation in the presence of GSK-J4 for 1.75 and 2 days showed at least 7 differentially phosphorylated ATM/ATR substrates compared to controls (Fig. 10A). Two prominent downstream targets of ATM/ATR are p53, which is phosphorylated at S15 (p-p53Ser15) in response to DNA damage, and H2AX, which marks DNA double strand break foci after phosphorylation at S139 (γH2AX) [128]. ES cells treated with DMSO, GSK-J5 or GSK-J4 showed constant levels of p-p53Ser15, p53 and γH2AX. Compared to undifferentiated ES cells differentiating ES cells in the presence of GSK-J4 showed strongly increased protein levels of p53, p-p53Ser15 and γH2AX (Fig. 10B). In accordance with published literature [129, 130] basal γH2AX levels were higher in undifferentiated ES cells then in differentiating ES cells.

The results indicate that in GSK-J4-treated differentiating ES cells key components of the DDR are increased.

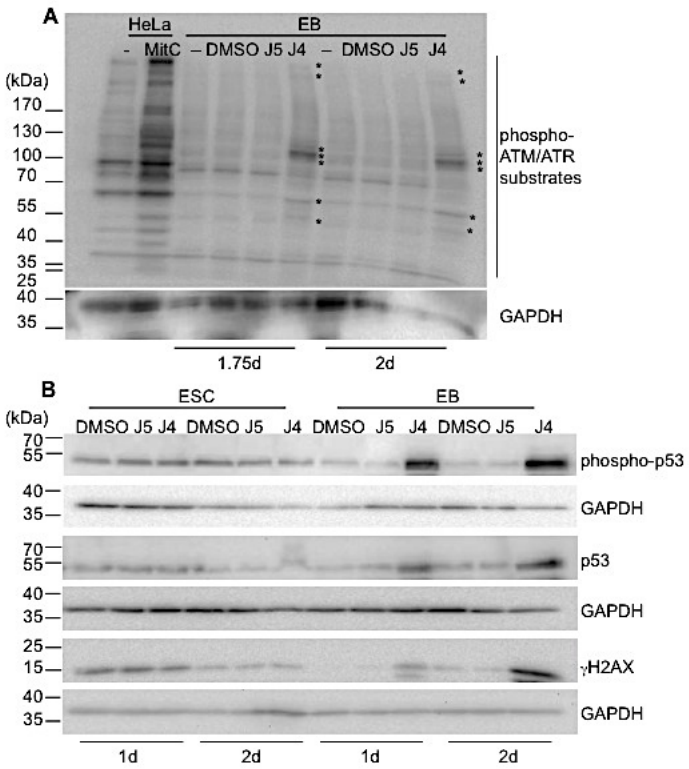

Fig. 10: Inhibition of KDM6A and KDM6B induces DNA damage signaling in differentiating ES cells. A) Western blot analyses of differentiating ES cells cultured in the presence of differentiation medium only (-), DMSO, GSK-J5 or GSK-J4 for indicated periods. Protein extracts of HeLa cells and MitC-treated HeLa cells served as positive controls. Blots were probed with antibodies specific for phospho-ATM/ATR substrates and GAPDH (loading control). Asterisks indicate ATM/ATR substrates phosphorylated in response to GSK-J4 treatment. B) Western blot analyses of undifferentiated and differentiating ES cells that were cultured in the presence of DMSO, GSK-J5 or GSK-J4 (1 or 2 days). Membranes were probed with antibodies specific for phospho-p53 (Ser15), p53, γH2AX (Ser 139) and GAPDH (loading control). A), B) All experiments were performed with R1 cells.

From the literature it is known that mouse ES cells display elevated basal levels of γH2AX even in the absence of double strand breaks (DSB) or single strand breaks (SSB) [129, 130]. To find out if differentiation of ES cells in the presence of GSK-J4 led to DNA damage Comet Assays were performed (by J. M. Kampka, AG Mueller). Comet Assays confirmed that in the presence of GSK-J4 differentiating ES cells accumulated DNA damage comparable to DNA damage that was observed after exposure of EBs to a dose of 6Gy IR.

3.3 KDM6B Knock down in KDM6A Knock out ES cells

To rule out off-target effects sometimes paralleling inhibitor treatments KDM6A and KDM6B was genetically ablated. Therefore, a KDM6B KD in KDM6A KO ES cells was performed. Two validated lentiviral shRNAs for KDM6B (#1 and #2) and one lentiviral shRNA targeting a non-mammalian region (scr., scrambled) were employed. WT and KDM6A KO ES cells transducted with the scr. shRNA served as controls.

3.3.1 KDM6A KO/ KDM6B KD does not effect undifferentiated ES cells

Lentiviral transduction experiments were performed to investigate whether undifferentiated KDM6A KO/KDM6B KD ES cells show similar features like ES cells, which were treated with GSK-J4. First KDM6B KD in KDM6A KO ES cells was verified on RNA level. KDM6B KD efficiency ranged between 33 - 40% (Fig. 11A). Immunofluorescence (IF) stainings, using a KDM6B-specific antibody, confirmed the KD on protein level (Fig. 11B). The KD of KDM6B in KDM6A KO ES cells showed no effect on cell viability (Fig. 11C) and did not change cell cycle phase distribution (Fig. 11D). Furthermore, the level of SSEA-1 positive cells was not altered in KDM6A KO/KDM6B KD cells compared to control cells (Fig. 11E). Finally, the frequency of apoptotic ES cells was similar in WT, KDM6A KO or KDM6A KO/KDM6B KD ES cells (Fig. 11E).
Based on these analyses undifferentiated KDM6A KO/KDM6B KD ES cells showed no alterations compared to WT or KDM6A KO ES cells.

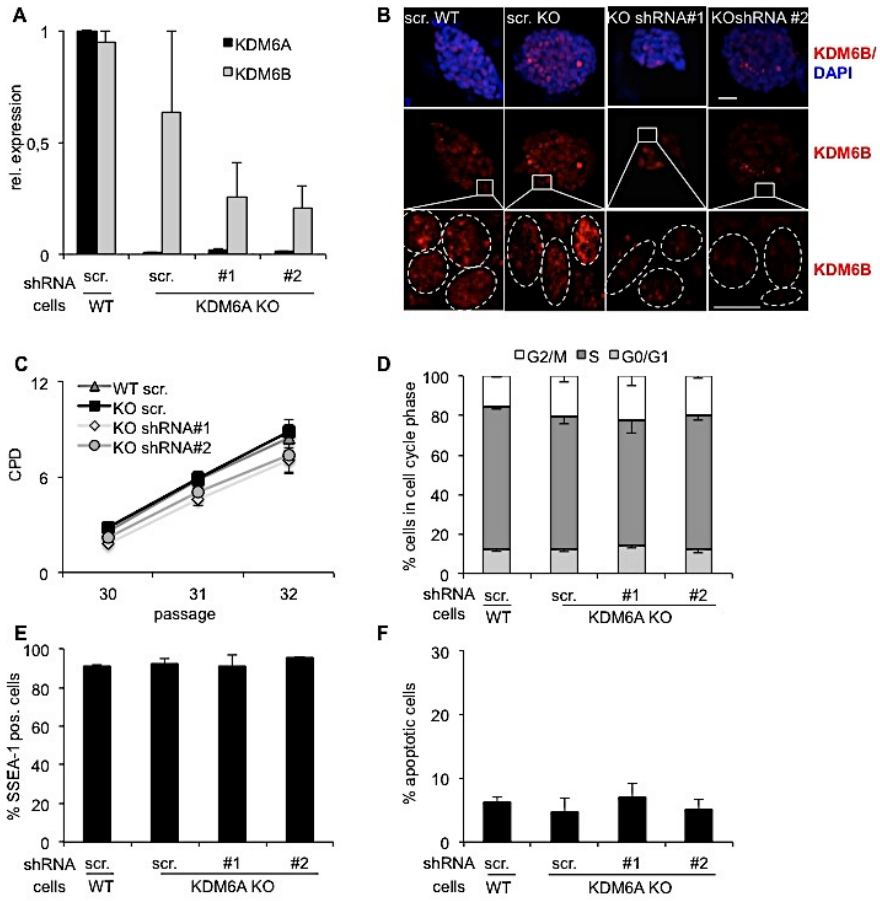

Fig. 11: KDM6A KO/KDM6B KD shows no effect on undifferentiated ES cells. A) Undifferentiated KDM6A KO ES cells were transduced with lentiviral shRNAs coding for a scrambled (scr.) or two different KDM6B sequences (shRNA#1, shRNA#2). 4 days after selection qRT-PCR analyses were performed to determine the expression of KDM6A and KDM6B in undifferentiated ES cells. Expression levels were normalized to GAPDH and RPL4. B) IF stainings of undifferentiated ES cells grown on MEFs were fixed after 4 days of selection and probed with an antibody specific for KDM6B and DAPI. Scale bar = 10 µm. Segment magnifications of areas marked by white squares are shown in the lower panel. White dashed lines mark nuclear perimeters. Scale bar = 5 µm. C) CPD of undifferentiated ES cells (WT, KDM6A KO and KDM6A KO/KDM6B KD) cultured for three passages. D) 4 days after selection undifferentiated ES cells were subjected to PI/FACS analyses for quantification of percentages of cells in G0/G1-, S- or G2/M-phase. E) SSEA-1 staining of undifferentiated ES cells 4 days after selection. F) Fraction of apoptotic cells 4 days after selection. Single cell suspensions were analyzed by combined 7-AAD/Annexin V staining. A), C) - F) Shown are means of 2 independent experiments. Error bars represent SEM. All experiments were performed with KDM6A KO cells of a R1 ES cell background.

3.3.2 KDM6B KD in differentiating KDM6A KO ES cells reduces proliferation, increases apoptosis and activates DDR

KDM6A KO/KDM6B KD ES cells were differentiated to investigate whether differentiating KDM6A KO/KDM6B KD cells show similar features like differentiating ES cells, which were treated with GSK-J4.

To confirm KDM6B KD in 3 day-old differentiating KDM6A KO ES cells expression analyses were performed (Fig. 12A). The efficiency of the KDM6B KD in differentiating KDM6A KO ES cells was ~ 86 - 90%. Differentiation of KDM6A KO/KDM6B KD ES cells compared to control cells showed reduced PD levels (Fig. 12B). A two- to four-fold increased frequency of apoptotic cells in 1 or 2 day-old KDM6A KO/KDM6B KD differentiating ES cells was detected (Fig. 12C). The diameters of EBs were 10 - 30% reduced (Fig. 12D). Similar to ES cells, which were differentiated in the presence of GSK-J4, 3 day-old differentiating KDM6A KO/KDM6B KD ES cells showed a slight G0/G1-phase arrest (Fig. 12E). Finally the activity of p-p53Ser15 and γH2AX was increased in differentiating KDM6A KO/KDM6B KD ES cells compared to appropriate controls (Fig. 12F).

In summary, differentiating KDM6A KO/KDM6B KD ES cells showed similar characteristics compared to cells, which were differentiated in the presence of GSK-J4.

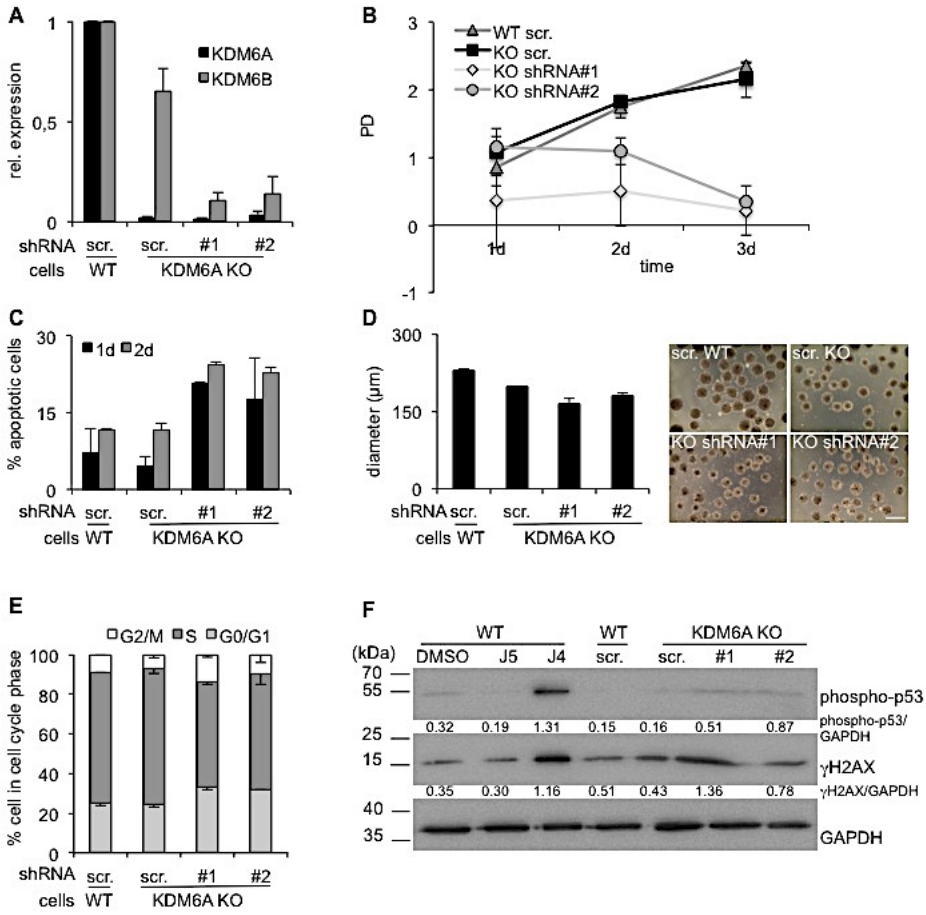

Fig. 12: KDM6B KD in differentiating KDM6A KO ES cells leads to reduced proliferation, increased apoptosis and activated DDR. A) Gene expression of KDM6A and KDM6B in 3 day-old differentiating KDM6A KO/KDM6B KD ES cell cultures. Expression levels were normalized to GAPDH and RPL4. B) PD of differentiating ES cells (WT, KDM6A KO or KDM6A KO/KDM6B KD) in suspension cultures (2x10^6 undifferentiated ES cells seeded at day 0). Cell numbers were determined at the indicated time points. C) Fraction of apoptotic cells. Single cell suspensions of 1 or 2 day-old differentiating ES cells were analysed by combined 7-AAD/Annexin V staining. D) Diameter of 3 day-old EBs (in µm) of KDM6B KD in a KDM6A KO and control cells (left graph) and micrographs of 3 day-old EBs (right). Scale bar = 500 µm. E) Single cell suspensions of 3 day-old differentiating ES cells were subjected to PI/FACS analyses for quantification of percentages of cells in G0/G1-, S- or G2/M-phase. A) - E) Shown are means of 2 independent experiments. Error bars represent SEM. F) Western blot analyses of WT differentiating ES cells cultured in the presence of DMSO, GSK-J5 or GSK-J4 for 2 days (left) or 3 day-old differentiating ES cells of WT, KDM6A KO or KDM6A KO/KDM6B KD (right). Membranes were probed with antibodies specific for phospho-p53 (Ser15), γH2AX and GAPDH (loading control). Numbers below blots indicate levels relative to GAPDH as determined by densitometric analyses. A) – F) All experiments were performed with KDM6A KO cells of a R1 ES cell background.

3.4 No co-localisation of H3K27me3 or KMD6B and γH2AX foci

In order to analyse if GSK-J4 treatment in undifferentiated and differentiating ES cells leads to changes in the localization of H3K27me3 or KDM6B IF stainings were performed. Double stainings were applied to identify if H3K27me3 or KDM6B co-localized with γH2AX foci.

Consistent with results from Fig. 4A elevated H3K27me3 levels were found in GSK-J4 treated undifferentiated and differentiating ES cells (Fig. 13A, lower panels). As depicted in Fig. 10B higher frequencies of γH2AX foci in GSK-J5 treated undifferentiated ES cells compared to GSK-J5 treated differentiating ES cells were noticed (Fig. 13A and 13B, upper panels). A co-localization of H3K27me3 with γH2AX foci in undifferentiated and differentiating ES cells was not detected in GSK-J5 or GSK-J4 treated cells (Fig. 13A). Since H3K27me3 levels of GSK-J4 treated undifferentiated and differentiating ES cells were increased, more overlay of H3K27me3 and γH2AX signals were seen (Fig. 13A, lower panels). KDM6B was in the presence of GSK-J5 or GSK-J4 in undifferentiated and differentiating ES cells localized to the nucleus and cytoplasm (Fig. 13B). A co-localization of KDM6B and γH2AX foci was not detected in any of the samples. Since KDM6A and KDM6B inhibition, as part of its DNA damaging action, might altered the localization of KDM6B undifferentiated and differentiating ES cells with irradiation-induced DNA damage were used as controls. These cells were exposed to a dose of 6Gy of IR based on the results of the Comet Assays. Upon IR no increased H3K27me3 levels (Fig. 13C) or altered KDM6B subcellular localization (Fig. 13D) was detected in undifferentiated or differentiating ES cells. Further, no co-localisation of H3K27me3 or KDM6B with γH2AX foci was detected upon irradiation-induced DNA damage.

In summary, a co-localization of H3K27me3 or KDM6B and γH2AX foci was not observed. Besides that, subcellular localization of KDM6B remained unaltered in response to GSK-J4 or IR.

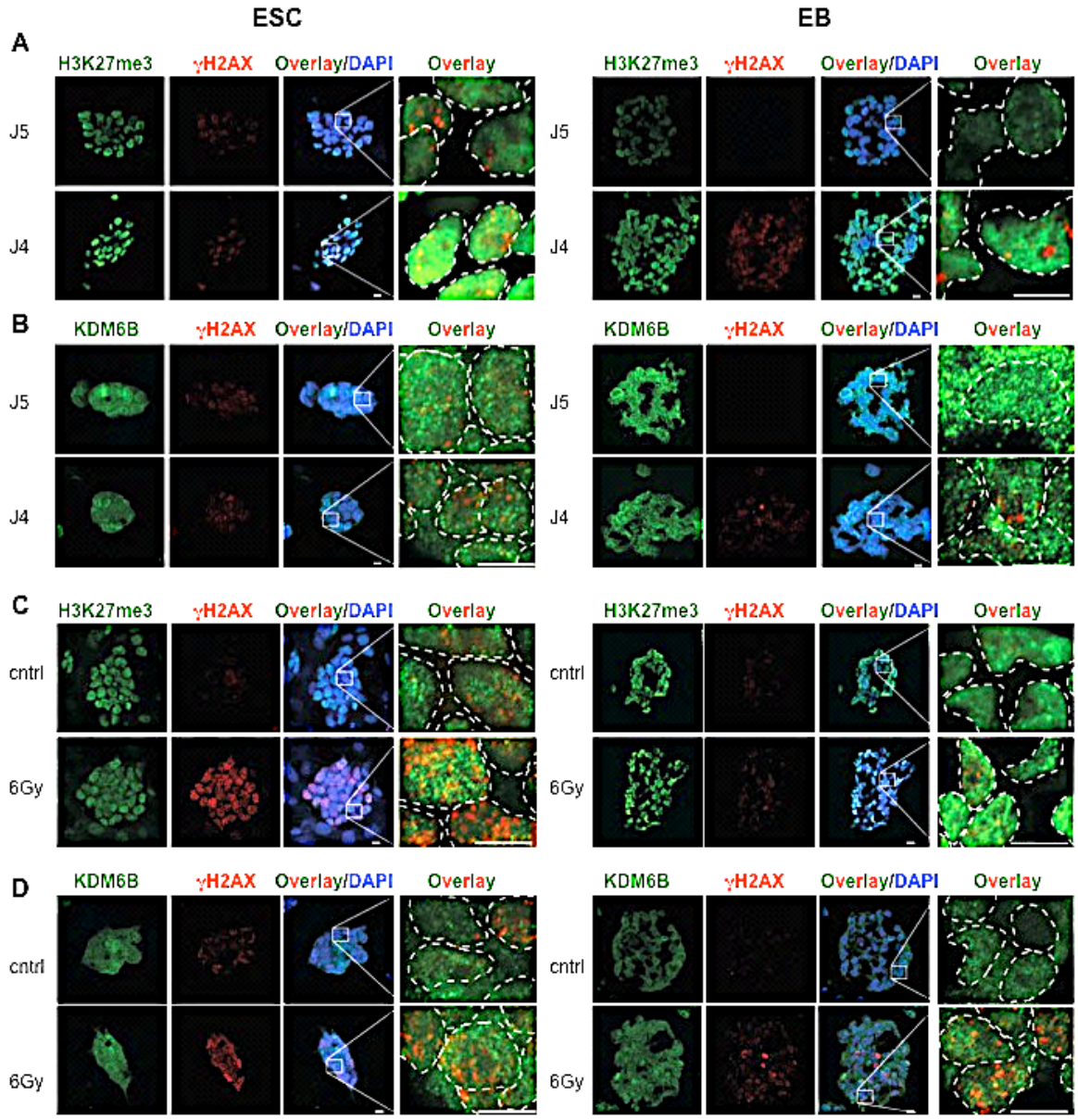

Fig. 13: Subcellular distribution of H3K27me3, γH2AX foci, and localization of KDM6B upon GSK-J4 treatment or IR exposure. A), B) IF stainings of undifferentiated ES cells (ESC) cultured for 2 days or differentiating ES cells (EB) cultured for 0.75 day in the presence of GSK-J5 or GSK-J4. C), D) IF stainings of undifferentiated or differentiating ES cells were left untreated (cntrl) or exposed to 6Gy IR (6Gy). Undifferentiated ES cells were cultured for 2 days and differentiating ES cells were cultured for 0.75 day prior IR exposure. A) - D) Undifferentiated or differentiating ES cells were probed with antibodies specific for H3K27me3 and γH2AX or KDM6B and γH2AX, nuclei were stained with DAPI. Undifferentiated ES cells are shown in left panels, EBs are shown in right panels ”Overlay”-images represent segment magnifications of areas marked by white squares in the “Overlay/DAPI”-images. White dashed lines mark nuclear perimeters. Scale bar = 10 µm in “Overlay”-images and 5 µm in ”Overlay/DAPI”-images respectively. All experiments were performed with R1 ES cells.

3.5 Lack of H3K27me3 attenuates GSK-J4-induced DDR in differentiating Eed KO ES cells

As depicted in Fig. 4C ES cell differentiation in the presence of GSK-J4 was indispensible. If differentiation was impaired due to globally increased H3K27me3 levels or by enzymatic inhibition of KDM6A and KDM6B through GSK-J4 was not clear. To get more information about the role of the H3K27me3 mark Eed KO ES cells, which lack H3K27me3, were used.

3.5.1 Expression of KDM6A and KDM6B in undifferentiated and differentiating WT and Eed KO ES cells

To confirm the KO of Eed and to investigate if Eed KO cells, which lack H3K27me3 marks, express H3K27me3-specific demethylases expression analyses on RNA and protein levels using undifferentiated and differentiating ES cells were performed. WT (J1) ES cells served as controls.

The expression of Eed in WT cells decreased upon differentiation while undifferentiated and differentiating Eed KO ES cells lacked Eed expression (Fig. 14A). As depicted in Fig. 14B undifferentiated Eed KO ES cells were devoid of Eed and H3K27me3 while WT ES cells showed basal protein levels of Eed and H3K27me3. Finally, KDM6A- and KDM6B-specific qRT-PCRs using undifferentiated and differentiating WT and Eed KO ES cells were performed (Fig. 14C). Undifferentiated and differentiating Eed KO ES cells expressed KDM6A and KDM6B at similar levels as WT ES cells. The expression level of KDM6A slightly decreased upon differentiation while KDM6B expression remained unaffected.

These data indicate, that undifferentiated and differentiating Eed KO ES cells expressed H3K27me3-specific demethylases at similar levels as WT cells.

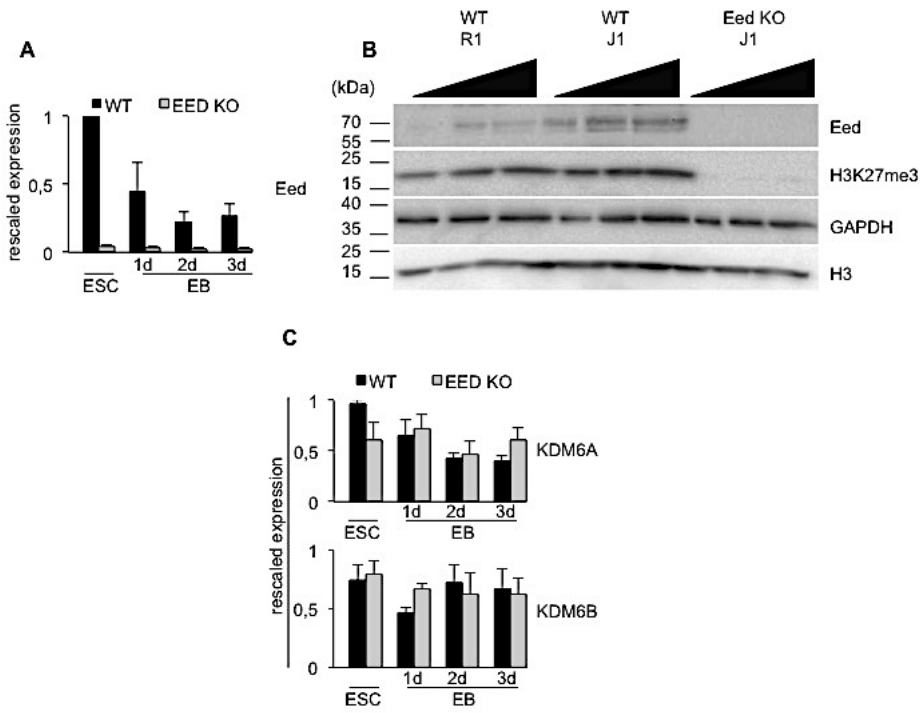

Fig. 14: Expression of Eed, KDM6A and KDM6B in undifferentiated and differentiating WT and Eed KO ES cells. A) qRT-PCR expression analyses of Eed in undifferentiated or differentiating WT J1 or Eed KO (J1) ES cells. B) Western blot analyses of undifferentiated ES cells (wt lines: R1, J1 and Eed KO line (J1)). Blots were probed with antibodies specific for Eed, H3K27me3, GAPDH and H3 (two loading controls). C) qRT-PCR expression analyses of KDM6A or KDM6B in WT J1 or Eed KO (J1) ES cells and EBs (1, 2 and 3 days). A), C) Expression levels were normalized to GAPDH and RPL4. Shown are means of three independent experiments. Error bars represent SEM.

3.5.2 Absence of Eed attenuates the GSK-J4 effect on cell viability and proliferation in differentiating ES cells

Next, differentiation experiments of Eed KO ES cells, in the presence of GSK-J4, were carried out to assess the influence of the H3K27me3/2-specific demethylase inhibitor on differentiating ES cells, which lack H3K27me3 marks.

Differentiation of Eed KO ES cells in the presence of GSK-J4 was moderately affected in contrast to WT (R1, J1) ES cells (Fig. 15A) and cellularity of differentiating ES cells showed a mild decline in differentiating Eed KO ES cells compared to WT (J1) cells (Fig. 15B).

In summary, the absence of Eed attenuated the GSK-J4 effect on cell viability and proliferation in differentiating ES cells.

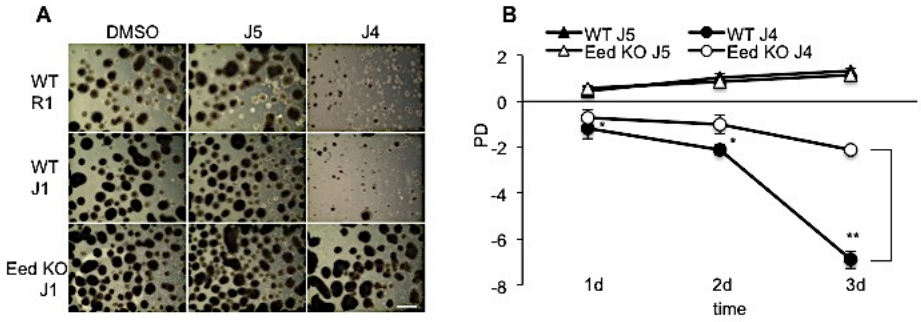

Fig. 15: Differentiation of Eed KO ES cell in the presence of GSK-J4. A) Representative micrographs of differentiating WT R1, WT J1 and Eed KO (J1) ES cells in the presence of DMSO, GSK-J5 or GSK-J4 for 3 days in suspension cultures (2x10^6 cells seeded at day 0). Scale bar = 500 µm. B) PD of differentiating WT J1 and Eed KO (J1) ES cells in suspension cultures (2x10^6 cells seeded at day 0) and cultured for up to 3 days in the presence of GSK-J5 or GSK-J4. Shown are mean of 3 independent experiments. Error bars represent SEM. *: p≤ 0.05; **: p≤ 0.01. Experiments were performed with WT (J1) and Eed KO (J1) ES cells.

3.5.3 Eed KO cells show a reduced frequency of γH2AX foci when differentiated in the presence of GSK-J4

As described in the previous chapter, the absence of Eed attenuated the GSK-J4 effect in differentiating ES cells. To find out if the attenuated GSK-J4 effect is due to reduced DNA damage, the frequency of γH2AX foci in differentiating Eed KO ES cells after GSK-J5 or GSK-J4 treatments were determined. WT cells served as controls.
In differentiating GSK-J5 treated Eed KO ES cells a moderate increased fraction of cells with γH2AX foci was noticed compared to differentiating GSK-J5 treated WT ES cells (Fig. 16). The amount of γH2AX foci in differentiating GSK-J4 treated Eed KO ES cells were markedly lower compared to differentiating GSK-J4 treated WT ES cells.
These results support the notion that differentiating Eed KO ES cells in the presence of GSK-J4 developed less DNA damage.

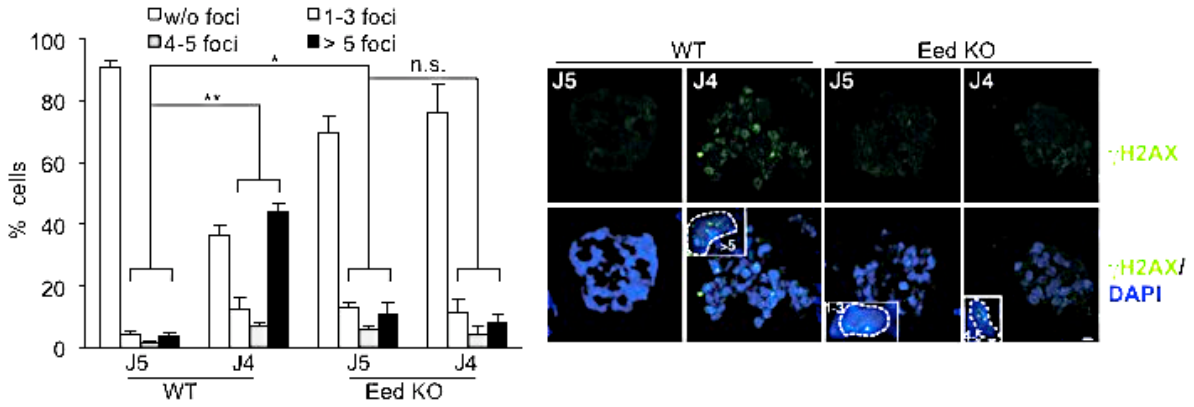

Fig. 16: Eed KO cells show a reduced frequency of γH2AX foci when differentiated in the presence GSK-J4. γH2AX-specific IF analyses were performed to analyze the frequency of γH2AX foci in GSK-J5/GSK-J4 treated differentiating ES cells (left graph). Representative micrographs are shown (right) of 0.75 day differentiating ES cells. Shown are means of three independent experiments. Scale bar = 10 µm. Error bars represent SEM. *: p≤ 0.05; **: p≤ 0.01, n. s. no significance. Experiments were performed with differentiating WT (J1) and Eed KO (J1) ES cells.

3.6 Expression of Ku70/Ku80 in undifferentiated and differentiating ES cells

The heterodimer Ku70/Ku80 recruits DNA repair kinases to DNA lesions, which repair DNA DSBs by non-homologous end joining (NHEJ) [131]. To investigate if under GSK-J4 treatment the proteins Ku70/Ku80, which are necessary for DNA DSB repair, are differentially expressed expression analyses of Ku70/Ku80 in undifferentiated and differentiating ES cells were performed.

Undifferentiated ES cells showed no altered Ku70 or Ku80 RNA expression in the presence of GSK-J4. Interestingly, in the presence of GSK-J4 differentiating ES cells showed a decreased RNA expression of Ku70, while expression of Ku80 increased until day 2 and declined on day 3 of differentiation (Fig. 17A).

In line with the RNA expression analyses protein expression of Ku80 in undifferentiated ES cells were at constant levels. In contrast to the RNA expression 1 and 2 day-old differentiating ES cells showed a declined Ku80 protein expression under GSK-J4 treatment (Fig. 17B). The results show that KDM6A and KDM6B inhibition upon differentiation led to decreased Ku80 protein expression.

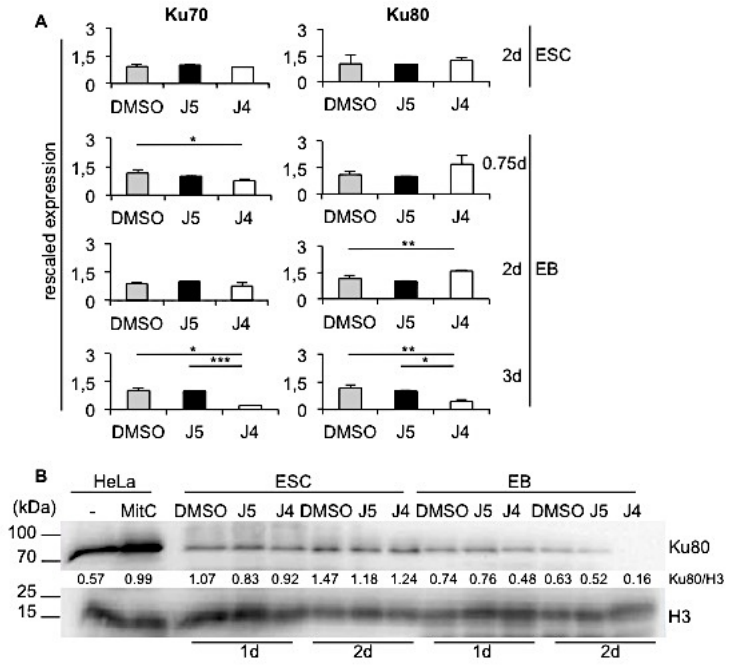

Fig. 17: Expression of Ku70/Ku80 in undifferentiated and differentiating ES cells. A) Undifferentiated or differentiating ES cells were treated for the indicated periods with DMSO, GSK-J5 or GSK-J4 before RNA was prepared and qRT-PCR was performed. Expression levels were normalized to GAPDH and RPL4. Shown are means of three independent experiments. Error bars represent SEM. *: p≤ 0.05 **: p≤ 0.01 ***: p≤ 0.001. B) Western blot analyses of undifferentiated or differentiating ES cells cultured in the presence of DMSO, GSK-J5 or GSK-J4 (for 1 or 2 days) and probed with antibodies specific for Ku80 and H3 (loading control). HeLa cells either left untreated or incubated with MitC served as a positive control. Numbers below blots indicate levels relative to H3 as determined by densitometric analyses. Shown are means of two independent blots out of two independent experiments. A), B) All experiments were performed with R1 ES cells.

3.7 Inhibition of KDM6A and KDM6B enzymatic activities reduces hematopoietic colony formation

To characterize the effects of a complete inhibition of the enzymatic KDM6A and KDM6B activity on hematopoietic progenitor cells colony forming assays were performed. To this end freshly murine BM cells were seeded into clonogenic methylcellulose cultures supplemented with myelo/erthroid growth factors and GSK-J4, GSK-J5 or DMSO.

A two- to three-fold reduced colony formation under GSK-J4 treatment was analyzed (Fig.18, left) going along with a reduced cellularity within these colonies (Fig. 18, right).

These results led to the conclusion that hematopoietic progenitor cells in the presence of GSK-J4 have a reduced colony forming potential.

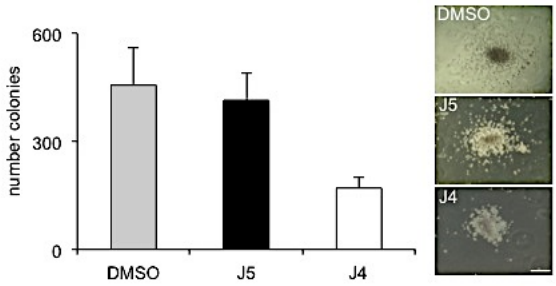

Fig. 18: Differentiation of BM isolated cells in the presence of GSK-J4. Freshly isolated BM cells of male mice were differentiated in the presence of DMSO, GSK-J5 or GSK-J4. After 4 days developing BL-CFCs were counted (right) and micrographs of colonies at day 4 are shown (left). Scale bar = 500 µm. Shown are means of three independent experiments performed in triplicates. Error bars represent SEM.

4. Discussion

The aim of this thesis was to characterise the role of the H3K27me3/2-specific histone demethylases KDM6A and KDM6B in undifferentiated and differentiating ES cells. To this end a specific KDM6A and KDM6B inhibitor (GSK-J4), as well as KDM6A KO/KDM6B KD ES cells were employed.
Unexpectedly, I found that inhibition of KDM6A and KDM6B led to cell death in early differentiating, but not in undifferentiated ES cells. Global gene expression analyses in differentiating ES cells revealed that only a limited set of genes was differentially regulated in response to GSK-J4 treatment with more genes up-regulated than down-regulated. Several of the up-regulated genes encode factors associated with DDR. Consistently, GSK-J4 incubation caused severe DNA damage, which preceded G1-phase arrest and cell death. Co-localization of H3K27me3 or KDM6B with γH2AX foci marking DNA double strand breaks was not observed. However, lack of H3K27me3 attenuated GSK-J4-induced DDR in differentiating Eed KO ES cells. Finally, hematopoietic differentiation in the presence of GSK-J4 resulted in a reduced colony-forming potential. The following paragraphs will discuss the results.

4.1 Role of KDM6A and KDM6B in the Regulation of H3K27me3 Levels in Differentiating ES Cells

In this study the simultaneous inhibition of KDM6A and KDM6B led to globally increased H3K27me3 levels in undifferentiated and differentiating ES cells while H3K27me2 levels remained unaltered (Fig. 3, 4). Why are global H3K27me3 levels increased while H3K27me2 levels remain uneffected? So far nobody ever analysed global H3K27me3 and K3K27me2 levels in mouse ES cells with a combined enzymatic loss of KDM6A and KDM6B. Individual KO of KDM6A or KDM6B in mouse ES cells did not alter global H3K27me3 and K3K27me2 levels [80, 83, 84, 132]. It was shown that the Jmj catalytic domain and the zinc-binding domain, only found in KDM6 family members, confer target specificity [133, 134]. With this it is likely that KDM6 family members compensate for each other. Kruidenier *et al.* showed that the

inhibitor GSK-J4 is selective for the H3K27 demethylases KDM6A and KDM6B and is inactive against a panel of demethylases of the JMJ family, including KDM6C [99].
Data from Walport *et al.* just recently showed that KDM6C catalyses demethylation of H3K27 peptides *in vitro*, analogously to KDM6A and KDM6B, but with reduced activity [135]. KDM6A, KDM6B and KDM6C are so far the only identified H3K27me3-specific demethylases [35, 73-75, 135] while besides KDM6 family members one additional H3K27me2-specific demethylase (KDM7A) is known [76, 136]. Upon GSK-J4 treatment KDM6C and KDM7A might compensate the enzymatic inhibition of the H3K27me2-specific demethylases KDM6A and KDM6B. This may explain why GSK-J4 treatment leads to globally increased H3K27me3 levels and unaltered H3K27me2 levels.

4.2 Inhibition of KDM6A and KDM6B Affects Gene Regulation in Differentiating ES Cells

Although higher global H3K27me3 levels were observed in differentiating ES cells in response to GSK-J4 treatment only a relatively small number of genes (303) were differentially expressed. In contrast to what could be expected after global up-regulation of a repressive chromatin mark the majority of genes (221) were expressed at higher levels (Fig. 9).
Based on these results two questions arise: Why is the number of differentially expressed genes so low and why are more genes up-regulated than down-regulated?
The relatively low number of differentially regulated genes could be explained by findings from Pauler *et al.* [137]. Pauler and colleagues performed ChIP-chip analyses and found, that the majority of H3K27me3 modifications preferentially form broad local enrichments (BLOCs) in gene-rich regions. H3K27me3 BLOCs do not specifically mark promoters, but are rather equally distributed among genes and intergenic regions. Many H3K27me3 BLOCs are localized within silenced genes while active genes are mostly devoid of H3K27me3 BLOCs [137]. The location of H3K27me3-enriched regions in GSK-J4 treated ES cells was not determined. With this it cannot be ruled out that H3K27me3 modifications are increased in regions,

which are not essential for gene regulation in undifferentiated and differentiating ES cells. Cell stress could have caused the fraction of the observed gene expression changes. In accordance with published literature stating an up-regulation of KDM6B in response to stress signals [69, 138] an increased KDM6B expression in response to GSK-J4 treatment was noticed in differentiating ES cell (Fig. 5). Additionally, many genes associated with DNA damage and DDR were up-regulated in response to GSK-J4 treatment (Fig. 9, 10, 13) at a time point where DNA damage was already evident in differentiating ES cells treated with GSK-J4.

4.3 Role of KDM6A and KDM6B in DNA Damage

In response to GSK-J4 treatment DNA damage and induction of a DDR were detected in differentiating ES cell cultures (Fig. 9, 10, 13) while the lack of H3K27me3 attenuates GSK-J4 induced DDR in differentiating Eed KO ES cells (Fig. 16).

Until now several histone demethylases could be linked to DNA damage or to DDR [139-144]. KDM1A for instance binds to sites of DNA damage and reduces H3K4 dimethyl marks at these sites while the loss of KDM1A makes cells hypersensitive to DNA damage [141]. The key question is: How are the proteins KDM6A and KDM6B and/or the H3K27me3 mark linked to DNA damage?

Co-localization of KDM6B and γH2AX foci in undifferentiated or differentiating ES cells was not found (Fig. 13). These results confirm findings from Mosammaparast and colleagues [141] who report that KDM6B is not located at sites of DNA damage. The sub-nuclear localization of KDM6A was not analysed although it seems unlikely that KDM6A co-localized with γH2AX foci as KO of KDM6A in differentiating ES cells did not induce DNA damage (Fig. 12). To elucidate the function of H3K27me3 in DNA damage and DDR WT ES cells and Eed KO ES cells, which lack H3K27me3 marks, were treated with GSK-J4.

It is known that members of the PRC1 and PRC2 complexes are recruited to sites of DSB [145]. Data on PRC function during DDR suggest that PRC play a role downstream of ATM [146]. Consistently, sensitization to IR and UV were reported as a consequence of deletion of PRC1 or PRC2 components like Bmi1 and Ezh2 [147, 148]. In agreement with an increased sensitivity to DNA damage higher frequencies

of γH2AX foci were found in differentiating Eed KO ES cells compared to differentiating WT ES cells (Fig. 16). The frequency of γH2AX foci in the presence of GSK-J4 in differentiating Eed KO ES cells was reduced compared to WT ES cells (Fig. 16). While two recent studies showed increased H3K27me3 at UV light-induced DNA damage sites [148, 149] two other studies revealed no co-localization in response to UV or IR exposure [147, 150]. This discrepancy may derive from varying experimental conditions. Exposure to IR did not increase H3K27me3 levels in undifferentiated or differentiating ES cells (Fig. 13). After GSK-J4 treatment or exposure to IR co-localization of H3K27me3 and γH2AX foci in undifferentiated and differentiating WT ES cells was not detected (Fig. 13).

Based on these observations KDM6A and KDM6B might play an indirect role in the acquisition of DNA damage. Findings from Williams and colleagues support this notion [151]. They reported that the transcription factor and tumour suppressor p53 interacts with KDM6B [151]. KDM6B binds to p53 target sites, which regulate genes involved in cell cycle regulation, response to stress and apoptosis [69, 138, 151]. Further, they show that in response to IR-induced DNA damage the expression of KDM6B, p53, p-p53Ser15 and the binding of KDM6B to p53 target sites is increased [151]. In agreement with results from Williams *et al.* an increased expression of KDM6B, p53 and p-p53Ser15 was found in differentiating ES cells, which show in response to GSK-J4 DNA damage (Fig. 5, 10). Nevertheless, the binding of KDM6B to p53 target sites was not analysed in differentiating ES cells in the presence of GSK-J4.
It can be hypothesized that upon DNA damage H3K27me3 marks need to be depleted to de-repress p53 target genes, which function in response to DNA damage. In the presence of GSK-J4 p53 target genes are potentially repressed which could cause a failed DDR and finally an increased frequency of apoptotic cells. Thus, H3K27me3/2-specific demethylase activity might be essential for the activation of genes in response to DNA damage. To prove this hypothesis the location of increased H3K27me3 in response to GSK-J4 needs to be identified with *e.g.* the Chip-Seq. analysis of H3K27me3.

But why does the lack of H3K27me3 attenuate GSK-J4 induced DDR specifically in differentiating Eed KO ES cells? As discussed above the demethylase activity of

KDM6A and KDM6B is potentially essential to remove H3K27me3 at promoter regions of genes associated with DDR. It is known that cells lacking H3K27me3 show an increased expression of PRC2 target genes [152]. It can therefore be assumed that upon DNA damage Eed KO cells are constantly able to express DNA damage- and DDR-associated genes, resulting in a reduced rate of apoptotic cells.

4.4 Repair Mechanism in Undifferentiated and Differentiating ES Cells

Treatment with GSK-J4 had no effect on the viability or proliferation on ES cells while ES cell differentiation was completely abrogated in the presence of GSK-J4 (Fig. 4, 6 - 8). The most interesting question is: Why do differentiating ES cells accumulate DNA damage in response to KDM6A and KDM6B inhibition while undifferentiated ES cells show no response upon GSK-J4 treatment?

A possible cause could be de-regulation of a cellular process such as replication. Stalled replication forks elicit DNA damage signalling [153] along with intra S-cell cycle arrest [154]. My work, however, shows enrichment of GSK-J4 treated cells in the G1-cell cycle phase (Fig. 7). Therefore I do not consider stalled replication forks as a likely reason for DNA damage in differentiating ES cells in response to KDM6A and KDM6B inhibition. Inefficient repair of basal DNA damage could be another possible reason for the accumulation of DNA lesions. Seminal studies revealed that undifferentiated ES cells are distinct from differentiating cells with respect to DDR [155, 156]. Undifferentiated ES cells for example express base excision repair (BER) and mismatch repair (MMR) factors at higher levels than differentiated MEFs [155, 156]. DSB and SSB are the most frequent forms of DNA damage [157]. While undifferentiated ES cells preferentially repair DNA breaks by homologous recombination (HR) differentiated cells favour the error prone non-homologous end joining (NHEJ) [158]. Data on DNA repair mechanism during early ES cell differentiation do not exist. It is however tempting to speculate that KDM6A and KDM6B may play a role in the transition from a preferential use of HR in undifferentiated ES cells towards NHEJ preferentially used in differentiated cells. In this context the co-presence of PTIP and KDM6A or KDM6B in the MLL2 complex may be of relevance [50]. PTIP also interacts with 53BP1 and has recently been

shown to be required for 53BP1-mediated inhibition of HR [108]. So far, it is not known whether KDM6A or KDM6B are involved in PTIP mediated inhibition of HR.
A role for KDM6A in NHEJ in *Drosophila* has recently been published [131]. During NHEJ DSBs are marked by Ku70/Ku80 proteins, which recruit repair factors to the DNA lesion [142]. Zhang *et al.* observed that upon IR induced DNA damage KDM6A removes H3K27me3 marks at the Ku80 promoter resulting in an upregulation of Ku80. Upon DNA damage the expression of Ku70 increased as well, though the regulation of Ku70 was not dependent on KDM6A activity. Upon IR induced DNA damage KDM6A KD cells were no longer able to remove the H3K27me3 mark at the Ku80 promoter and an upregulation of Ku80 was impeded [142]. Although I observed a reduced protein level of Ku80 in differentiating ES cells treated with GSK-J4 RNA expression analyses of Ku70/Ku80 are inconsistent with data from Zhang *et al.* (Fig. 17). This transcriptional discrepancy may derive from varying experimental conditions.

4.5 Inhibition of KDM6A and KDM6B Effects Hematopoietic Differentiation

When murine BM cells were differentiated in the presence of GSK-J4 a reduced colony-forming ability was observed (Fig. 18). Based on these results the question arises: Why is the hematopoietic colony-forming ability in the presence of GSK-J4 reduced? The reduced colony-forming ability could be explained by findings from Liu *et al.* [159]. Liu and colleagues performed a KDM6A KD in BM cells and found a reduced hematopoietic colony-forming ability. KDM6A is directly associates with promoters of mesodermal genes and modulates their transcription by controlling H3K27me3 marks on respective promoter regions [159]. In the presence of GSK-J4 KDM6A and KDM6B are enzymatically inactive. With this it seems likely that genes, which are essential for the hematopoietic differentiation, cannot be de-repressed resulting in a reduced hematopoietic colony formation. DNA damage could be another possible reason for the reduced hematopoietic colony-forming ability of BM cells in the presence of GSK-J4.

4.6 Conclusion

The results presented in my thesis demonstrate that the enzymatic activity of H3K27me3/2-specific demethylases KDM6A and KDM6B are not essential to maintain ES cell pluripotency. Instead, enzymatic activity of KDM6A and KDM6B are required for ES cell and hematopoietic differentiation. The inhibition of KDM6A and KDM6B in differentiating ES cells is associated with DNA damage, DDR and finally leads to apoptosis. Additional studies are needed to further assess the molecular function of KDM6A and KDM6B in differentiating ES cells and to identify their role in DNA damage and DDR.

Decreased expression and mutations of KDM6A and KDM6B are linked to altered histone modifications and to many types of cancer [60]. H3K27me3/2-specific inhibitors could represent new potential diagnostic tools as well as therapeutic targets in the field of oncology and could be of considerable interest as novel anticancer agents.

5. Abbreviations

7-AAD	7-amino-actinomycin D
ADP	adenosine diphosphate
AML	acute myeloid leukemia
AP	alkaline phosphatase
ATM	Ataxia telangiectasia mutated
ATR	Ataxia telangiectasia and Rad3-related
BL-CFC	blast colony-forming cells
BM	bone marrow
bp	base pair
BSA	bovine serum albumin
cDNA	copy deoxyribonucleic acid
CDS	coding sequence
cm	centimetre
cm^2	square centimetre
cntrl	Control
CPD	Cumulative Population Doublings
CpG	cytosine-guanine dinucleotides
CT	cycle threshold
Cy	cyanine
d	day(s)
DAPI	4',6-diamidino-2-phenylindole
DDR	DNA damage response
DMEM	Dulbecco's modified eagle medium
DMSO	dimethyl sulfoxide
DNA	deoxyribonucleic acid
DNMT	DNA methyltransferase
dNTP	deoxyribonucleotide triphosphate
DSB	DNA single strand break
EB	embryoid body
EDTA	ethylenediaminetetraacetic acid
Eed	embryonic ectoderm development
e.g.	*exempli gratia*, for example
Epo	erythropoietin
EtOH	ethyl alcohol

ES	embryonic stem
ESC	embryonic stem cell
et al.	*et alii*, and others
FACS	fluorescence activated cell sorting
FAD	flavin adenine dinucleotide
FCS	fetal calf serum
Fig.	figure
GM-CSF	granulocyte macrophage colony-stimulating factor
GO	Gene ontology
Gy	Gray
h	hour(s)
H	Histone
HBS	Hepes-buffered saline
HeLa	Henrietta Lacks
HDM	histone demethylase
HKMT	histone lysine methyltransferase
HMT	histone methyltransferase
HRP	horseradish peroxidase
HR	homologous recombination
Hox	Homeobox
ICM	inner cell mass (of blastocyst)
IF	Immunofluorescence
IL	interleukin
IMDM	Iscove's modified Dulbecco's medium
IR	ionizing irradiation
JARID2	Jumonji, AT rich interactive domain 2
JmjC	Jumonji C
Jmjd3	Jumonji D3
K	lysine
KD	knockdown
kDa	kiloDalton
KDM	histone lysine demethylase
KO	knockout
LIF	leukemia inhibitory factor
lncRNA	long noncoding ribonucleic acid
ng	nano gram
NHEJ	non-homologous end joining

n. s.	not significant
M	mol
MBD	methyl-CpG-binding domain
me	methylation
MEFs	mouse embryonic fibroblasts
min	minute
MitC	Mitomycin C
ml	millilitre
MLL	Mixed-lineage leukemia
mM	millimoles
mRNA	messenger ribonucleic acid
MTG	mono-thio glycerol
qRT-PCR	quantitative Real Time Polymerase chain reaction
P	p-value
PAGE	Polyacrylamide gel electrophoresis
PBS	phosphate buffered saline
PcG	Polycomb group
PD	Population Doubling
PFA	paraformaldehyde
pH	*potentia Hydrogenii*
PI	propidium iodide
pM	picomole
PRMT	protein arginine methyltransferase
PRC1	Polycomb repressive complex 1
PRC2	Polycomb repressive complex 2
pos.	positive
PVDF	polyvinyliden fluorid
R	arginine
rel.	relative
RNA	ribonucleic acid
rRNA	ribosomal ribonucleic acid
rpm	rounds per minute
RT	room temperature
s	second(s)
SCF	stem cell factor
scr	scrambled
SDS	sodium dodecyl sulfate

SDS-PAGE	sodium dodecyl sulfate polyacrylamide gel electrophorese
SEM	standard error of the mean
shRNA	small hairpin ribonucleic acid
SSB	Single strand break
SSEA-1	stage-specific embryonic antigen-1
STAT3	signal transducer and activator of transcription 3
TBS	tris-buffered saline
TC	tissue culture
TPR	tetratricopeptide repeats
TrxG	Trithorax group
U	unit
UTX	ubiquitously transcribed TPR gene on the X chromosome
UTY	ubiquitously transcribed TPR gene on the Y chromosome
w/o	without
WT	wild type
µl	micro litres
µm	micrometres
5mC	5-methylcytosine

6. References

1. Evans, M.J. and M.H. Kaufman, *Establishment in culture of pluripotential cells from mouse embryos.* Nature, 1981. **292**(5819): p. 154-6.
2. Martin, G.R., *Isolation of a pluripotent cell line from early mouse embryos cultured in medium conditioned by teratocarcinoma stem cells.* Proc Natl Acad Sci U S A, 1981. **78**(12): p. 7634-8.
3. Mitalipov, S. and D. Wolf, *Totipotency, pluripotency and nuclear reprogramming.* Adv Biochem Eng Biotechnol, 2009. **114**: p. 185-99.
4. Minguell, J.J., A. Erices, and P. Conget, *Mesenchymal stem cells.* Exp Biol Med (Maywood), 2001. **226**(6): p. 507-20.
5. Fuchs, E., T. Tumbar, and G. Guasch, *Socializing with the neighbors: stem cells and their niche.* Cell, 2004. **116**(6): p. 769-78.
6. Shahriyari, L. and N.L. Komarova, *Symmetric vs. asymmetric stem cell divisions: an adaptation against cancer?* PLoS One, 2013. **8**(10): p. e76195.
7. Thomson, J.A., et al., *Embryonic stem cell lines derived from human blastocysts.* Science, 1998. **282**(5391): p. 1145-7.
8. Thomson, J.A., et al., *Isolation of a primate embryonic stem cell line.* Proc Natl Acad Sci U S A, 1995. **92**(17): p. 7844-8.
9. Thomson, J.A., et al., *Pluripotent cell lines derived from common marmoset (Callithrix jacchus) blastocysts.* Biol Reprod, 1996. **55**(2): p. 254-9.
10. Vassilieva, S., et al., *Establishment of SSEA-1- and Oct-4-expressing rat embryonic stem-like cell lines and effects of cytokines of the IL-6 family on clonal growth.* Exp Cell Res, 2000. **258**(2): p. 361-73.
11. Williams, R.L., et al., *Myeloid leukaemia inhibitory factor maintains the developmental potential of embryonic stem cells.* Nature, 1988. **336**(6200): p. 684-7.
12. Wobus, A.M., et al., *Characterization of a pluripotent stem cell line derived from a mouse embryo.* Exp Cell Res, 1984. **152**(1): p. 212-9.
13. Kuijk, E.W., et al., *The different shades of mammalian pluripotent stem cells.* Hum Reprod Update, 2011. **17**(2): p. 254-71.
14. Hambiliki, F., et al., *Co-localization of NANOG and OCT4 in human pre-implantation embryos and in human embryonic stem cells.* J Assist Reprod Genet, 2012. **29**(10): p. 1021-8.
15. Wang, Z., et al., *Distinct lineage specification roles for NANOG, OCT4, and SOX2 in human embryonic stem cells.* Cell Stem Cell, 2012. **10**(4): p. 440-54.
16. Chambers, I. and S.R. Tomlinson, *The transcriptional foundation of pluripotency.* Development, 2009. **136**(14): p. 2311-22.
17. Di Stefano, B., et al., *An ES-like pluripotent state in FGF-dependent murine iPS cells.* PLoS One, 2010. **5**(12): p. e16092.
18. White, J. and S. Dalton, *Cell cycle control of embryonic stem cells.* Stem Cell Rev, 2005. **1**(2): p. 131-8.
19. Damjanov, I. and D. Solter, *Experimental teratoma.* Curr Top Pathol, 1974. **59**: p. 69-130.
20. Pluck, A. and C. Klasen, *Generation of chimeras by morula aggregation.* Methods Mol Biol, 2009. **561**: p. 219-29.
21. Boyer, L.A., et al., *Core transcriptional regulatory circuitry in human embryonic stem cells.* Cell, 2005. **122**(6): p. 947-56.

22. Christophersen, N.S. and K. Helin, *Epigenetic control of embryonic stem cell fate.* J Exp Med, 2010. **207**(11): p. 2287-95.
23. Scholer, H.R., et al., *Octamer binding proteins confer transcriptional activity in early mouse embryogenesis.* EMBO J, 1989. **8**(9): p. 2551-7.
24. Mitsui, K., et al., *The homeoprotein Nanog is required for maintenance of pluripotency in mouse epiblast and ES cells.* Cell, 2003. **113**(5): p. 631-42.
25. Chambers, I., et al., *Functional expression cloning of Nanog, a pluripotency sustaining factor in embryonic stem cells.* Cell, 2003. **113**(5): p. 643-55.
26. Avilion, A.A., et al., *Multipotent cell lineages in early mouse development depend on SOX2 function.* Genes Dev, 2003. **17**(1): p. 126-40.
27. Doetschman, T.C., et al., *The in vitro development of blastocyst-derived embryonic stem cell lines: formation of visceral yolk sac, blood islands and myocardium.* J Embryol Exp Morphol, 1985. **87**: p. 27-45.
28. Keller, G., et al., *Hematopoietic commitment during embryonic stem cell differentiation in culture.* Mol Cell Biol, 1993. **13**(1): p. 473-86.
29. Wartenberg, M., et al., *The embryoid body as a novel in vitro assay system for antiangiogenic agents.* Lab Invest, 1998. **78**(10): p. 1301-14.
30. Keller, G., *Embryonic stem cell differentiation: emergence of a new era in biology and medicine.* Genes Dev, 2005. **19**(10): p. 1129-55.
31. Desbaillets, I., et al., *Embryoid bodies: an in vitro model of mouse embryogenesis.* Exp Physiol, 2000. **85**(6): p. 645-51.
32. Surani, M.A., K. Hayashi, and P. Hajkova, *Genetic and epigenetic regulators of pluripotency.* Cell, 2007. **128**(4): p. 747-62.
33. Johnson, T. and R. Coghill, *Resarches on pyrimidines. C111 The discovery of 5-methyl-cytosine in tuberculinic acid, the nucleic acid of the tubercle bacillus.* J AM Chem Soc., 1925. **47**: p. 2838-44.
34. Liu, N. and T. Pan, *RNA epigenetics.* Transl Res, 2014.
35. Agger, K., et al., *UTX and JMJD3 are histone H3K27 demethylases involved in HOX gene regulation and development.* Nature, 2007. **449**(7163): p. 731-4.
36. Zhu, J.K., *Active DNA demethylation mediated by DNA glycosylases.* Annu Rev Genet, 2009. **43**: p. 143-66.
37. Razin, S.V. and A.A. Gavrilov, *Chromatin without the 30-nm fiber: Constrained disorder instead of hierarchical folding.* Epigenetics, 2014. **9**(5).
38. Luger, K., et al., *Crystal structure of the nucleosome core particle at 2.8 A resolution.* Nature, 1997. **389**(6648): p. 251-60.
39. Tamaru, H., *Confining euchromatin/heterochromatin territory: jumonji crosses the line.* Genes Dev, 2010. **24**(14): p. 1465-78.
40. Trojer, P. and D. Reinberg, *Facultative heterochromatin: is there a distinctive molecular signature?* Mol Cell, 2007. **28**(1): p. 1-13.
41. Hassa, P.O., et al., *Nuclear ADP-ribosylation reactions in mammalian cells: where are we today and where are we going?* Microbiol Mol Biol Rev, 2006. **70**(3): p. 789-829.
42. Sterner, D.E. and S.L. Berger, *Acetylation of histones and transcription-related factors.* Microbiol Mol Biol Rev, 2000. **64**(2): p. 435-59.
43. Zhang, Y. and D. Reinberg, *Transcription regulation by histone methylation: interplay between different covalent modifications of the core histone tails.* Genes Dev, 2001. **15**(18): p. 2343-60.
44. Nowak, S.J. and V.G. Corces, *Phosphorylation of histone H3: a balancing act between chromosome condensation and transcriptional activation.* Trends Genet, 2004. **20**(4): p. 214-20.

45. Shilatifard, A., *Chromatin modifications by methylation and ubiquitination: implications in the regulation of gene expression.* Annu Rev Biochem, 2006. **75**: p. 243-69.
46. Nathan, D., et al., *Histone sumoylation is a negative regulator in Saccharomyces cerevisiae and shows dynamic interplay with positive-acting histone modifications.* Genes Dev, 2006. **20**(8): p. 966-76.
47. Kanwal, R. and S. Gupta, *Epigenetic modifications in cancer.* Clin Genet, 2012. **81**(4): p. 303-11.
48. Cohen, I., et al., *Histone modifiers in cancer: friends or foes?* Genes Cancer, 2011. **2**(6): p. 631-47.
49. Grunstein, M., *Histone acetylation in chromatin structure and transcription.* Nature, 1997. **389**(6649): p. 349-52.
50. Cloos, P.A., et al., *Erasing the methyl mark: histone demethylases at the center of cellular differentiation and disease.* Genes Dev, 2008. **22**(9): p. 1115-40.
51. Nottke, A., M.P. Colaiacovo, and Y. Shi, *Developmental roles of the histone lysine demethylases.* Development, 2009. **136**(6): p. 879-89.
52. Bannister, A.J., R. Schneider, and T. Kouzarides, *Histone methylation: dynamic or static?* Cell, 2002. **109**(7): p. 801-6.
53. Blair, L.P., et al., *Epigenetic Regulation by Lysine Demethylase 5 (KDM5) Enzymes in Cancer.* Cancers (Basel), 2011. **3**(1): p. 1383-404.
54. Martin, C. and Y. Zhang, *The diverse functions of histone lysine methylation.* Nat Rev Mol Cell Biol, 2005. **6**(11): p. 838-49.
55. Shi, Y., et al., *Histone demethylation mediated by the nuclear amine oxidase homolog LSD1.* Cell, 2004. **119**(7): p. 941-53.
56. Hou, H. and H. Yu, *Structural insights into histone lysine demethylation.* Curr Opin Struct Biol, 2010. **20**(6): p. 739-48.
57. Peng, J.C., et al., *Jarid2/Jumonji coordinates control of PRC2 enzymatic activity and target gene occupancy in pluripotent cells.* Cell, 2009. **139**(7): p. 1290-302.
58. Takeuchi, T., et al., *Gene trap capture of a novel mouse gene, jumonji, required for neural tube formation.* Genes Dev, 1995. **9**(10): p. 1211-22.
59. Trewick, S.C., P.J. McLaughlin, and R.C. Allshire, *Methylation: lost in hydroxylation?* EMBO Rep, 2005. **6**(4): p. 315-20.
60. Rotili, D. and A. Mai, *Targeting Histone Demethylases: A New Avenue for the Fight against Cancer.* Genes Cancer, 2011. **2**(6): p. 663-79.
61. Shirato, H., et al., *A jumonji (Jarid2) protein complex represses cyclin D1 expression by methylation of histone H3-K9.* J Biol Chem, 2009. **284**(2): p. 733-9.
62. Lan, F., A.C. Nottke, and Y. Shi, *Mechanisms involved in the regulation of histone lysine demethylases.* Curr Opin Cell Biol, 2008. **20**(3): p. 316-25.
63. Hayami, S., et al., *Overexpression of LSD1 contributes to human carcinogenesis through chromatin regulation in various cancers.* Int J Cancer, 2011. **128**(3): p. 574-86.
64. Suzuki, T., et al., *Tumor suppressor gene identification using retroviral insertional mutagenesis in Blm-deficient mice.* EMBO J, 2006. **25**(14): p. 3422-31.
65. Pfau, R., et al., *Members of a family of JmjC domain-containing oncoproteins immortalize embryonic fibroblasts via a JmjC domain-dependent process.* Proc Natl Acad Sci U S A, 2008. **105**(6): p. 1907-12.

66. Hu, Z., et al., *A novel nuclear protein, 5qNCA (LOC51780) is a candidate for the myeloid leukemia tumor suppressor gene on chromosome 5 band q31.* Oncogene, 2001. **20**(47): p. 6946-54.
67. Cloos, P.A., et al., *The putative oncogene GASC1 demethylates tri- and dimethylated lysine 9 on histone H3.* Nature, 2006. **442**(7100): p. 307-11.
68. Zeng, J., et al., *The histone demethylase RBP2 Is overexpressed in gastric cancer and its inhibition triggers senescence of cancer cells.* Gastroenterology, 2010. **138**(3): p. 981-92.
69. Agger, K., et al., *The H3K27me3 demethylase JMJD3 contributes to the activation of the INK4A-ARF locus in response to oncogene- and stress-induced senescence.* Genes Dev, 2009. **23**(10): p. 1171-6.
70. Greenfield, A., et al., *The UTX gene escapes X inactivation in mice and humans.* Hum Mol Genet, 1998. **7**(4): p. 737-42.
71. Greenfield, A., et al., *An H-YDb epitope is encoded by a novel mouse Y chromosome gene.* Nat Genet, 1996. **14**(4): p. 474-8.
72. Lee, S., J.W. Lee, and S.K. Lee, *UTX, a histone H3-lysine 27 demethylase, acts as a critical switch to activate the cardiac developmental program.* Dev Cell, 2012. **22**(1): p. 25-37.
73. Lan, F., et al., *A histone H3 lysine 27 demethylase regulates animal posterior development.* Nature, 2007. **449**(7163): p. 689-94.
74. Lee, M.G., et al., *Demethylation of H3K27 regulates polycomb recruitment and H2A ubiquitination.* Science, 2007. **318**(5849): p. 447-50.
75. De Santa, F., et al., *The histone H3 lysine-27 demethylase Jmjd3 links inflammation to inhibition of polycomb-mediated gene silencing.* Cell, 2007. **130**(6): p. 1083-94.
76. Walport, L.J., et al., *Human UTY(KDM6C) is a Male-Specific N{epsilon}-Methyl Lysyl-Demethylase.* J Biol Chem, 2014.
77. Morales Torres, C., A. Laugesen, and K. Helin, *Utx is required for proper induction of ectoderm and mesoderm during differentiation of embryonic stem cells.* PLoS One, 2013. **8**(4): p. e60020.
78. Hong, S., et al., *Identification of JmjC domain-containing UTX and JMJD3 as histone H3 lysine 27 demethylases.* Proc Natl Acad Sci U S A, 2007. **104**(47): p. 18439-44.
79. Welstead, G.G., et al., *X-linked H3K27me3 demethylase Utx is required for embryonic development in a sex-specific manner.* Proc Natl Acad Sci U S A, 2012. **109**(32): p. 13004-9.
80. Shpargel, K.B., et al., *UTX and UTY demonstrate histone demethylase-independent function in mouse embryonic development.* PLoS Genet, 2012. **8**(9): p. e1002964.
81. Blatch, G.L. and M. Lassle, *The tetratricopeptide repeat: a structural motif mediating protein-protein interactions.* Bioessays, 1999. **21**(11): p. 932-9.
82. Cho, Y.W., et al., *PTIP associates with MLL3- and MLL4-containing histone H3 lysine 4 methyltransferase complex.* J Biol Chem, 2007. **282**(28): p. 20395-406.
83. Thieme, S., et al., *The histone demethylase UTX regulates stem cell migration and hematopoiesis.* Blood, 2013. **121**(13): p. 2462-73.
84. Wang, C., et al., *UTX regulates mesoderm differentiation of embryonic stem cells independent of H3K27 demethylase activity.* Proc Natl Acad Sci U S A, 2012. **109**(38): p. 15324-9.

85. Vandamme, J., et al., *The C. elegans H3K27 demethylase UTX-1 is essential for normal development, independent of its enzymatic activity.* PLoS Genet, 2012. **8**(5): p. e1002647.
86. Smith, E.R., et al., *Drosophila UTX is a histone H3 Lys27 demethylase that colocalizes with the elongating form of RNA polymerase II.* Mol Cell Biol, 2008. **28**(3): p. 1041-6.
87. Denton, D., et al., *UTX coordinates steroid hormone-mediated autophagy and cell death.* Nat Commun, 2013. **4**: p. 2916.
88. Lee, H.Y., et al., *HIF-1-Dependent Induction of Jumonji Domain-Containing Protein (JMJD) 3 under Hypoxic Conditions.* Mol Cells, 2014. **37**(1): p. 43-50.
89. Burgold, T., et al., *The histone H3 lysine 27-specific demethylase Jmjd3 is required for neural commitment.* PLoS One, 2008. **3**(8): p. e3034.
90. Burgold, T., et al., *The H3K27 demethylase JMJD3 is required for maintenance of the embryonic respiratory neuronal network, neonatal breathing, and survival.* Cell Rep, 2012. **2**(5): p. 1244-58.
91. Mansour, A.A., et al., *The H3K27 demethylase Utx regulates somatic and germ cell epigenetic reprogramming.* Nature, 2012. **488**(7411): p. 409-13.
92. Zhao, W., et al., *Jmjd3 inhibits reprogramming by upregulating expression of INK4a/Arf and targeting PHF20 for ubiquitination.* Cell, 2013. **152**(5): p. 1037-50.
93. Miyake, N., et al., *KDM6A point mutations cause Kabuki syndrome.* Hum Mutat, 2013. **34**(1): p. 108-10.
94. Kim, J.H., et al., *UTX and MLL4 Coordinately Regulate Transcriptional Programs for Cell Proliferation and Invasiveness in Breast Cancer Cells.* Cancer Res, 2014.
95. Xiang, Y., et al., *JMJD3 is a histone H3K27 demethylase.* Cell Res, 2007. **17**(10): p. 850-7.
96. Liu, J., et al., *Genome and transcriptome sequencing of lung cancers reveal diverse mutational and splicing events.* Genome Res, 2012. **22**(12): p. 2315-27.
97. van Haaften, G., et al., *Somatic mutations of the histone H3K27 demethylase gene UTX in human cancer.* Nat Genet, 2009. **41**(5): p. 521-3.
98. Ene, C.I., et al., *Histone demethylase Jumonji D3 (JMJD3) as a tumor suppressor by regulating p53 protein nuclear stabilization.* PLoS One, 2012. **7**(12): p. e51407.
99. Kruidenier, L., et al., *A selective jumonji H3K27 demethylase inhibitor modulates the proinflammatory macrophage response.* Nature, 2012. **488**(7411): p. 404-8.
100. Ang, Y.S., et al., *Wdr5 mediates self-renewal and reprogramming via the embryonic stem cell core transcriptional network.* Cell, 2011. **145**(2): p. 183-97.
101. Ingham, P.W., *A clonal analysis of the requirement for the trithorax gene in the diversification of segments in Drosophila.* J Embryol Exp Morphol, 1985. **89**: p. 349-65.
102. Tkachuk, D.C., S. Kohler, and M.L. Cleary, *Involvement of a homolog of Drosophila trithorax by 11q23 chromosomal translocations in acute leukemias.* Cell, 1992. **71**(4): p. 691-700.
103. Yu, B.D., et al., *Altered Hox expression and segmental identity in Mll-mutant mice.* Nature, 1995. **378**(6556): p. 505-8.
104. Bernstein, B.E., et al., *A bivalent chromatin structure marks key developmental genes in embryonic stem cells.* Cell, 2006. **125**(2): p. 315-26.

105. Xu, Z., et al., *The role of WDR5 in silencing human fetal globin gene expression.* Haematologica, 2012. **97**(11): p. 1632-40.
106. Wysocka, J., et al., *WDR5 associates with histone H3 methylated at K4 and is essential for H3 K4 methylation and vertebrate development.* Cell, 2005. **121**(6): p. 859-72.
107. Schwab, K.R., G.D. Smith, and G.R. Dressler, *Arrested spermatogenesis and evidence for DNA damage in PTIP mutant testes.* Dev Biol, 2013. **373**(1): p. 64-71.
108. Callen, E., et al., *53BP1 mediates productive and mutagenic DNA repair through distinct phosphoprotein interactions.* Cell, 2013. **153**(6): p. 1266-80.
109. Jowsey, P.A., A.J. Doherty, and J. Rouse, *Human PTIP facilitates ATM-mediated activation of p53 and promotes cellular resistance to ionizing radiation.* J Biol Chem, 2004. **279**(53): p. 55562-9.
110. Rowley, J.D., *The critical role of chromosome translocations in human leukemias.* Annu Rev Genet, 1998. **32**: p. 495-519.
111. Margueron, R. and D. Reinberg, *The Polycomb complex PRC2 and its mark in life.* Nature, 2011. **469**(7330): p. 343-9.
112. Aloia, L., B. Di Stefano, and L. Di Croce, *Polycomb complexes in stem cells and embryonic development.* Development, 2013. **140**(12): p. 2525-34.
113. Margueron, R., et al., *Role of the polycomb protein EED in the propagation of repressive histone marks.* Nature, 2009. **461**(7265): p. 762-7.
114. Shen, X., et al., *EZH1 mediates methylation on histone H3 lysine 27 and complements EZH2 in maintaining stem cell identity and executing pluripotency.* Mol Cell, 2008. **32**(4): p. 491-502.
115. Schuettengruber, B., et al., *Genome regulation by polycomb and trithorax proteins.* Cell, 2007. **128**(4): p. 735-45.
116. Dejardin, J., et al., *Recruitment of Drosophila Polycomb group proteins to chromatin by DSP1.* Nature, 2005. **434**(7032): p. 533-8.
117. Pasini, D., et al., *Suz12 is essential for mouse development and for EZH2 histone methyltransferase activity.* EMBO J, 2004. **23**(20): p. 4061-71.
118. Lee, T.I., et al., *Control of developmental regulators by Polycomb in human embryonic stem cells.* Cell, 2006. **125**(2): p. 301-13.
119. Pasini, D., et al., *The polycomb group protein Suz12 is required for embryonic stem cell differentiation.* Mol Cell Biol, 2007. **27**(10): p. 3769-79.
120. Chamberlain, S.J., D. Yee, and T. Magnuson, *Polycomb repressive complex 2 is dispensable for maintenance of embryonic stem cell pluripotency.* Stem Cells, 2008. **26**(6): p. 1496-505.
121. van der Stoop, P., et al., *Ubiquitin E3 ligase Ring1b/Rnf2 of polycomb repressive complex 1 contributes to stable maintenance of mouse embryonic stem cells.* PLoS One, 2008. **3**(5): p. e2235.
122. Faust, C., et al., *The eed mutation disrupts anterior mesoderm production in mice.* Development, 1995. **121**(2): p. 273-85.
123. O'Carroll, D., et al., *The polycomb-group gene Ezh2 is required for early mouse development.* Mol Cell Biol, 2001. **21**(13): p. 4330-6.
124. Montgomery, N.D., et al., *The murine polycomb group protein Eed is required for global histone H3 lysine-27 methylation.* Curr Biol, 2005. **15**(10): p. 942-7.
125. Ura, H., et al., *STAT3 and Oct-3/4 control histone modification through induction of Eed in embryonic stem cells.* J Biol Chem, 2008. **283**(15): p. 9713-23.

126. Cristofalo, V.J., et al., *Relationship between donor age and the replicative lifespan of human cells in culture: a reevaluation.* Proc Natl Acad Sci U S A, 1998. **95**(18): p. 10614-9.
127. Matsuoka, S., et al., *ATM and ATR substrate analysis reveals extensive protein networks responsive to DNA damage.* Science, 2007. **316**(5828): p. 1160-6.
128. Sengupta, S. and C.C. Harris, *p53: traffic cop at the crossroads of DNA repair and recombination.* Nat Rev Mol Cell Biol, 2005. **6**(1): p. 44-55.
129. Banath, J.P., et al., *Explanation for excessive DNA single-strand breaks and endogenous repair foci in pluripotent mouse embryonic stem cells.* Exp Cell Res, 2009. **315**(8): p. 1505-20.
130. Chuykin, I.A., et al., *Activation of DNA damage response signaling in mouse embryonic stem cells.* Cell Cycle, 2008. **7**(18): p. 2922-8.
131. Rivera-Calzada, A., et al., *Structural model of full-length human Ku70-Ku80 heterodimer and its recognition of DNA and DNA-PKcs.* EMBO Rep, 2007. **8**(1): p. 56-62.
132. De Santa, F., et al., *Jmjd3 contributes to the control of gene expression in LPS-activated macrophages.* EMBO J, 2009. **28**(21): p. 3341-52.
133. Kim, E. and J.J. Song, *Diverse ways to be specific: a novel Zn-binding domain confers substrate specificity to UTX/KDM6A histone H3 Lys 27 demethylase.* Genes Dev, 2011. **25**(21): p. 2223-6.
134. Sengoku, T. and S. Yokoyama, *Structural basis for histone H3 Lys 27 demethylation by UTX/KDM6A.* Genes Dev, 2011. **25**(21): p. 2266-77.
135. Walport, L.J., et al., *Human UTY(KDM6C) Is a Male-specific N-Methyl Lysyl Demethylase.* J Biol Chem, 2014. **289**(26): p. 18302-18313.
136. Huang, C., et al., *Dual-specificity histone demethylase KIAA1718 (KDM7A) regulates neural differentiation through FGF4.* Cell Res, 2010. **20**(2): p. 154-65.
137. Pauler, F.M., et al., *H3K27me3 forms BLOCs over silent genes and intergenic regions and specifies a histone banding pattern on a mouse autosomal chromosome.* Genome Res, 2009. **19**(2): p. 221-33.
138. Barradas, M., et al., *Histone demethylase JMJD3 contributes to epigenetic control of INK4a/ARF by oncogenic RAS.* Genes Dev, 2009. **23**(10): p. 1177-82.
139. Khoury-Haddad, H., et al., *PARP1-dependent recruitment of KDM4D histone demethylase to DNA damage sites promotes double-strand break repair.* Proc Natl Acad Sci U S A, 2014. **111**(7): p. E728-37.
140. Young, L.C., D.W. McDonald, and M.J. Hendzel, *Kdm4b histone demethylase is a DNA damage response protein and confers a survival advantage following gamma-irradiation.* J Biol Chem, 2013. **288**(29): p. 21376-88.
141. Mosammaparast, N., et al., *The histone demethylase LSD1/KDM1A promotes the DNA damage response.* J Cell Biol, 2013. **203**(3): p. 457-70.
142. Zhang, C., et al., *Drosophila UTX coordinates with p53 to regulate ku80 expression in response to DNA damage.* PLoS One, 2013. **8**(11): p. e78652.
143. Li, X., et al., *Histone demethylase KDM5B is a key regulator of genome stability.* Proc Natl Acad Sci U S A, 2014. **111**(19): p. 7096-101.
144. Polytarchou, C., et al., *The JmjC domain histone demethylase Ndy1 regulates redox homeostasis and protects cells from oxidative stress.* Mol Cell Biol, 2008. **28**(24): p. 7451-64.

145. Gieni, R.S., et al., *Polycomb group proteins in the DNA damage response: a link between radiation resistance and "stemness".* Cell Cycle, 2011. **10**(6): p. 883-94.
146. Vissers, J.H., M. van Lohuizen, and E. Citterio, *The emerging role of Polycomb repressors in the response to DNA damage.* J Cell Sci, 2012. **125**(Pt 17): p. 3939-48.
147. Campbell, S., et al., *Polycomb repressive complex 2 contributes to DNA double-strand break repair.* Cell Cycle, 2013. **12**(16): p. 2675-83.
148. Chou, D.M., et al., *A chromatin localization screen reveals poly (ADP ribose)-regulated recruitment of the repressive polycomb and NuRD complexes to sites of DNA damage.* Proc Natl Acad Sci U S A, 2010. **107**(43): p. 18475-80.
149. O'Hagan, H.M., H.P. Mohammad, and S.B. Baylin, *Double strand breaks can initiate gene silencing and SIRT1-dependent onset of DNA methylation in an exogenous promoter CpG island.* PLoS Genet, 2008. **4**(8): p. e1000155.
150. Sustackova, G., et al., *Acetylation-dependent nuclear arrangement and recruitment of BMI1 protein to UV-damaged chromatin.* J Cell Physiol, 2012. **227**(5): p. 1838-50.
151. Williams, K., et al., *The Histone Lysine Demethylase JMJD3/KDM6B Is Recruited to p53 Bound Promoters and Enhancer Elements in a p53 Dependent Manner.* PLoS One, 2014. **9**(5): p. e96545.
152. Boyer, L.A., et al., *Polycomb complexes repress developmental regulators in murine embryonic stem cells.* Nature, 2006. **441**(7091): p. 349-53.
153. Zeman, M.K. and K.A. Cimprich, *Causes and consequences of replication stress.* Nat Cell Biol, 2014. **16**(1): p. 2-9.
154. Dimitrova, D.S. and D.M. Gilbert, *Temporally coordinated assembly and disassembly of replication factories in the absence of DNA synthesis.* Nat Cell Biol, 2000. **2**(10): p. 686-94.
155. Maynard, S., et al., *Human embryonic stem cells have enhanced repair of multiple forms of DNA damage.* Stem Cells, 2008. **26**(9): p. 2266-74.
156. Tichy, E.D., et al., *Mismatch and base excision repair proficiency in murine embryonic stem cells.* DNA Repair (Amst), 2011. **10**(4): p. 445-51.
157. Polo, S.E. and S.P. Jackson, *Dynamics of DNA damage response proteins at DNA breaks: a focus on protein modifications.* Genes Dev, 2011. **25**(5): p. 409-33.
158. Tichy, E.D., et al., *Mouse embryonic stem cells, but not somatic cells, predominantly use homologous recombination to repair double-strand DNA breaks.* Stem Cells Dev, 2010. **19**(11): p. 1699-711.
159. Liu, J., et al., *A functional role for the histone demethylase UTX in normal and malignant hematopoietic cells.* Exp Hematol, 2012. **40**(6): p. 487-98 e3.

Supplement: Table 2

Differentially expressed genes of 0.75 day differentiated ES cells cultured in the presence of GSK-J4 vs. DMSO and GSK-J5

Down-regulated genes:

Affy. ID:	Symbol:	Affy. ID:	Symbol:
17239501	3110003A17Rik	17239664	Myb
17318118	9030619P08Rik	17532621	Ned3
17245581	A130077B15Rik	17301582	Nefl
17392690	Acss1	17233771	Neurog3
17395613	BC066135	17474708	Nlrp9b
17247852	Bcl11a	17479947	Olfr293
17497421	Bnip3	17493130	Olfr307
17364585	C330026H20Rik	17263187	Olfr318
17396152	Car3	17262551	Phf15
17254508	Car4	17526086	Pou2f3
17471222	Ccnd2	17418268	Pou3f1
17289971	Ccno	17541067	Rhox2g
17497076	Chst15	17476752	Rhpn2
17337852	Clic5	17458110	Rny3
17407496	Crct1	17219110	Rxrg
17279509	Crip1	17354299	Sema6a
17414984	D4Bwg0951e	17286365	Serpinb9
17281084	Egln3	17259534	Slc16a3
17516074	Esam	17266851	Slfn9
17485443	Fgf15	17251514	Snord118
17463338	Fgf23	17379389	Svs6
17439517	Fgf5	17340646	Tagap1
17544025	Fndc3c1	17232162	Vnn1
17259314	Fscn2	17277287	Vrtn
17450461	Gbp4	17373915	Wt1
17415292	Gm13271	17354411	Zfp608
17464530	Gm20559		
17513232	Gm9564		
17344642	H2-T10		
17403004	H2afz		
17433461	Hes3		
17285938	Hist1h2aa		
17291258	Hist1h2ba		
17255620	Hoxb1		
17284614	Ighg3		
17467519	Igkv8-30		
17370883	Kcnj3		
17477362	Klk1b24		
17515315	Ldlr		
17402662	Lef1		
17392047	Lrrn4		
17480922	Mir139		
17315198	Mir1941		
17328220	Mir1945		
17291026	Mir1983		
17402479	Mir302a		
17402477	Mir302c		
17491699	Mir344d-2		
17362941	Ms4a14		

Up-regulated genes:

Affy. ID:	Symbol:	Affy. ID:	Symbol:
17526929	1110032A03Rik	17411420	Cth
17383373	1700007K13Rik	17265268	Cxcl16
17250734	2410006H16Rik	17494739	Cyb5r2
17346923	2410021H03Rik	17365001	Cyp2c44
17437380	9230114K14Rik	17331692	Cyyr1
17465608	AB041803	17223852	D630023F18Rik
17434555	Abcb1b	17237978	Ddit3
17277134	Acot2	17241032	Ddit4
17430288	Adc	17402996	Ddit4l
17314115	Adm2	17335281	Def6
17215576	Agap1	17308842	Dgkh
17547719	Ahnak2	17223002	Dnahc7a
17426277	Akna	17309457	Dzip1
17243544	Aldh1l2	17407001	Efna3
17265193	Alox12	17369925	Eng
17522504	Als2cl	17230484	Ephx1
17389161	Ano3	17431282	Extl1
17244140	Apaf1	17538683	Fam120c
17470580	Apobec1	17384205	Fam125b
17448174	Arap2	17218186	Fam129a
17399112	Arhgef2	17428050	Fam159a
17428996	Artn	17318249	Fam83h
17231033	Atf3	17324332	Fetub
17490391	Atf5	17493949	Folr2
17266581	AU040972	17232649	Fyn
17371912	B230120H23Rik	17510114	Gdf15
17268243	B4galnt2	17527977	Glce
17474097	Bbc3	17244961	Glipr1l3
17519364	BC031353	17413500	Glipr2
17427802	BC055111	17335726	Glp1r
17320499	BC090627	17406165	Glrb
17472760	Bhlhe41	17217562	Gm10535
17428752	Btbd19	17391781	Gm14057
17227089	Btg2	17377703	Gm14164
17239528	Ccdc28a	17345722	Gm14873
17531183	Ccdc36	17342996	Gm16197
17356427	Ccdc85b	17540739	Gm2012
17226622	Cd55	17290214	Gm20251
17373825	Cd59a	17483058	Gm20367
17373817	Cd59b	17535054	Gm364
17325608	Cd80	17305297	Gm3676
17356754	Cdc42bpg	17487635	Gm4567
17335467	Cdkn1a	17287957	Gm4934
17379938	Cebpb	17341170	Gm5091
17446767	Cgref1	17518553	Gm514
17374807	Chac1	17325329	Gm5483
17376119	Chchd5	17540741	Gm6121
17548664	Cln8	17442834	Gpr133
17293721	Cntnap3	17248191	Gpr75
17367278	Commd3	17446851	Gtf3c2
17496857	Cox6a2	17307801	Gulo
17437129	Cpeb2	17502789	Gypa
17490481	Cpt1c		
17388332	Creb3l1		
17332181	Cryzl1		

Affy. ID:	Symbol:	Affy. ID:	Symbol:
17510772	Hhip	17313721	Parvg
17285746	Hist1h2bn	17548046	Pcdhga10
17500451	Hmgb1-rs17	17300504	Pck2
17451629	Hnf1a	17393022	Pdrg1
17466798	Hoxa1	17231844	Perp
17441524	Hrk	17217619	Phlda3
17256513	Hsd17b1	17224971	Pid1
17519868	Htr1b	17420546	Pla2g2e
17521428	Hyal1	17289794	Plk2
17518458	Igdcc4	17217083	Pm20d1
17245890	Inhbe	17295212	Polk
17277396	Jdp2	17326510	Pros1
17217969	Kcnt2	17314699	Prph
17313000	Kdelr3	17453124	Psph
17275890	Klhdc1	17218060	Ptgs2
17510057	Klhl26	17220724	Ptpn14
17240538	Lace1	17224551	Ptprn
17228136	Lamc2	17397962	Rap2b
17419287	Laptm5	17449562	Rassf6
17547231	LOC100039574	17308568	Rb1
17547256	LOC100040744	17503756	Rbl2
17546255	LOC100862038	17214759	Rhbdd1
17285846	LOC100862646	17272437	Rhbdf2
17341148	LOC106740	17361276	Rhod
17546461	LOC382133	17317031	Samd12
17351133	LOC545261	17489464	Scn1b
17280062	Lpin1	17291736	Serpinb6c
17336965	Ly6g5c	17224771	Serpine2
17302754	Mbnl2	17493658	Serpinh1
17516518	Mcam	17227311	Shisa4
17343088	Mdga1	17260869	Slc1a4
17226953	Mdm4	17486956	Slc1a5
17501828	Mef2b	17509976	Slc25a42
17315007	Mettl7a3	17391709	Slc4a11
17541699	Mir19b-2	17417702	Slc6a9
17368067	Mir3087	17455401	Slc7a1
17278814	Mir323	17405082	Slc7a11
17278810	Mir380	17376510	Smox
17543813	Mir421	17541917	Snord61
17255947	Mir5119	17252845	Snord91a
17262355	Mir804	17361638	Snx32
17298825	Mmrn2	17315312	Soat2
17232215	Moxd1	17412593	Srsf12
17519821	Myo6	17546425	Srsy
17295627	Naip1	17546450	Ssty2
17477508	Napsa	17261425	Stc2
17361805	Neat1	17445440	Steap1
17387267	Neurod1	17242535	Syde1
17281306	Nkx2-9	17544469	Taf7l
17496345	Nupr1	17306816	Tgm1
17357788	Olfr1431	17245044	Tmem19
17278188	Otub2	17392925	Trib3
17387542	P2rx3	17494868	Trim66
17442149	P2rx4	17411751	Trp53inp1
		17345293	Vegfa
		17358422	Vldlr

Affy. ID:	Symbol:
17489997	Vmn2r57
17252292	Wscd1
17405365	Wwtr1
17466003	Zc3hav1
17219897	Zfp238
17241646	Zfp365
17273536	Zfp750
17536339	Zxdb

Permission from Genes and Development

Genes & Development

From: Christine Hofstetter <christine.hofstetter@uni-wuerzburg.de>
Sent: Thursday, May 01, 2014 1:09 PM
To: Genes & Development
Subject: Copyright - Christine Hofstetter

Dear editorial office employee,

for my doctoral thesis I would like to use a Figures (Parts of Fig. 2 and Fig. 3) from following Review:

Cloos, P.A., et al., Erasing the methyl mark: histone demethylases at the center of cellular differentiation and disease. Genes Dev, 2008.
22(9): p. 1115-40.

Whom can I ask for the copyright? Do I contact the authors directl?

Thanks a lot and greetings from Germany
Christine Hofstetter

Permission granted by the copyright owner, contingent upon the consent of the original author, provided complete credit is given to the original source and copyright date.

By Christina Kary, Ph.D. 5/13/14
Date

COLD SPRING HARBOR LABORATORY PRESS

Affidavit

I hereby declare that my thesis entitled

Inhibition of H3K27-specific demethylase activity during murine ES cell differentiation induces DNA damage response

is the result of my own work. I did not receive any help or support from commercial consultants.

All sources and / or materials used are listed or specified in the thesis.

Furthermore, I verify that this entire thesis or any part of its contents has not been submitted or is not under consideration for another examination process, neither in identical nor in similar form.

Place, Date ..... Signature .....

Hereby it is confirmed that I worked on my own on the following parts of my doctoral thesis:

ES cell culture, RNA isolation, qRT-PCR-based expression analyses, analyses of apoptosis, cell cycle distribution, Western blot analyses, AP stainings, FACS analyses, immunofluorescence stainings and analyses, lentiviral transduction experiments, BM cell isolation and hematopoietic differentiation.

Fig. 9: For global gene expression analysis, I cultivated cells and isolated RNAs. Microarray preparation and determination of gene expression levels were performed by Dr. Heike Weber, Microarray-Gruppe, IZKF Würzburg.

Christine Hofstetter

Place, Date Wü, 10.7.2014 *Signature* .....

Prof. Dr. Albrecht Müller

Place, Date Wü, 10.07.2014 *Signature* .....

A manuscript with the title '**Inhibition of H3K27-specific demethylase activity during murine ES cell differentiation induces DNA damage'** by Christine Hofstetter, Justyna M. Kampka, Heike Weber, Albrecht M. Müller, and Matthias Becker has been submitted.